6-28-2018

Demonstration of the Gas Assisted Gravity Drainage (GAGD) Process in Carbonate Rocks.

Alok Jiteshkumar Shah
Louisiana State University and Agricultural and Mechanical College, ashah18@lsu.edu

DEMONSTRATION OF THE GAS ASSISTED GRAVITY DRAINAGE (GAGD) PROCESS IN CARBONATE ROCKS

A Thesis

Submitted to the Graduate Faculty of the
Louisiana State University and
Agricultural and Mechanical College
in partial fulfillment of the
requirements for the degree of
Master of Science

in

The Craft and Hawkins Department of Petroleum Engineering

by
Alok Jiteshkumar Shah
B.S. (Environmental Engineering), University of Georgia, 2013
August 2018

ACKNOWLEDGEMENTS

I would like to express major gratitude to my advisor Dr. Dandina N. Rao, whose constant encouragement, feedback and ideas were of paramount value towards the completion of this work. I am also very thankful to Dr. Seung Kam and Dr. Ipsita Gupta of the Petroleum Engineering Department for their valuable suggestions and for serving on my thesis examination committee. Also, Dr. Mileva Radonjic provided useful comments and feedback for my project.

Further, I would like to recognize the availability of the LIFT funds from the LSU board of regents for providing me with financial support while pursuing my masters at Louisiana State University. The mechanical engineering department's Advanced Manufacturing and Machining Facility was instrumental in fabricating the equipment used for my research and especially Mr. Nic Dinecola was extremely helpful for the equipment used for this experiment. I would also like to recognize Mr. Fenelon Nunes of the Petroleum Engineering department for being available day and night for any lab supplies and support throughout my masters. I would also like to thank my friends and colleagues for their support and guidance throughout my time at LSU, in particular Iskandar Dzulkarnain, Ali Al Isawi, Bikash Saikia and Foad Haeri.

Finally, I would like to thank my family who has provided me with great encouragement, support and love throughout this process.

TABLE OF CONTENTS

LIST OF TABLES

LIST OF FIGURES

SYMBOLS AND ABBREVIATIONS

A = area of the porous medium

D_p = the grain size diameter

g = the gravitational acceleration

g_c = a gravitational acceleration conversion factor

h = the height of the porous medium

K = the absolute permeability of the porous medium

K_{ro}^{o} = End-point relative oil permeability

L = length of the porous medium

N_B = the Bond number

N_C = the capillary number

N_G = the gravity number

PVI = Pore Volume Injected

S_{or} = the residual oil saturation

S_{wi} = the initial water saturation

T_D = dimensionless time

V_p = pore volume

V_b = bulk volume

$\Delta\rho$ = the density difference between the two fluids

φ = the porosity of the porous medium

μ = viscosity of the fluid

ν = the Darcy velocity

τ = the tortuosity of the flow path through the porous medium

ABSTRACT

The Gas Assisted Gravity Drainage (GAGD) process was developed and patented by Dr. Rao at LSU in the early 2000s. The process involves the use of several existing or new vertical injection wells to inject gas and use the natural segregation of reservoir fluids from the density difference and the gravitational forces to displace the trapped oil and mobilize the oil downwards to be produced by a horizontal producing well. The GAGD process can be implemented as a secondary or tertiary oil recovery method. Several physical model experiments have been conducted to demonstrate the effectiveness of the GAGD process for improving oil recovery.

This research study is to expand the existing knowledge of the GAGD process and to apply it for carbonate rocks as more than 60% of world's oil is held in carbonate reservoirs. In particular, this study focuses on the impact of type of gas injected, injection rate of gas, and the grain size of the porous media. A glass model similar to a Hele-Shaw type model was used for performing the experiments using carbonate rocks as the porous media, water and n-decane for oil. The results from this study show that using nitrogen gas provides slightly higher recovery for the GAGD process in carbonate rocks compared to carbon dioxide. Further, the optimal injection rate is at an intermediate injection rate that doesn't disturb the stable front which can create an earlier breakthrough at higher injection rates. Finally, the larger grain size shows a significant improvement in overall oil recovery since increasing grain size diameter increases permeability and thus better overall oil recovery is obtained. The oil recovery from this study ranges from 70.9% to 87.7% of OOIP.

1. INTRODUCTION

Oil has been a fundamental ingredient to the human lifestyle development over the last century. It has enabled some of the most vital improvements in the industrialized society and their impacts can't be understated. The extraction and recovery of oil is through three main stages; primary recovery, secondary and tertiary recovery. Enhanced Oil Recovery (EOR) processes involve injection of a fluid into a reservoir that supplements the natural energy of a reservoir to produce the remaining oil in a reservoir (Rao, 2012). EOR methods are employed following primary and secondary recovery in hydrocarbon reservoirs to extract the remaining oil in place from a reservoir. Several different methods exist to extract the remaining oil such as chemical flooding, thermal recovery, gas flooding, etc. One such method is the Gas Assisted Gravity Drainage (GAGD). GAGD is an EOR method, invented and patented, at the Louisiana State University EOR lab (Rao, 2012). The process involves the use of several existing or new vertical injection wells to pump gas and use natural gravity segregation to displace the trapped oil and mobilize the oil downwards to be produced by a horizontal producing well. The basic idea behind the process is to take advantage of the natural segregation of different density mixtures to allow for gas injection from top while collection of oil at the bottom of the pay zone. A general schematic of the process is shown in Figure 1.1 below (Rao et al, 2006).

Previous studies have been conducted on the GAGD process especially on lab scale models to test various parameters that affect the performance of the process and to determine the optimal parameter sequence as discussed in the literature review section below. However, not much prior work has yet been undertaken for the feasibility of GAGD in carbonate reservoirs.

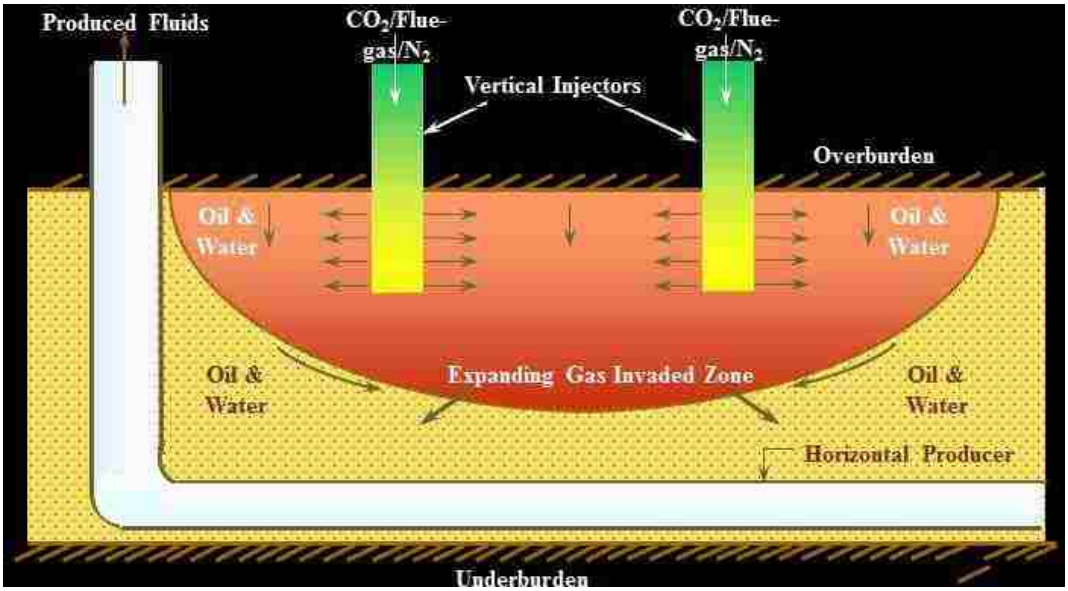

Figure 1.1. General schematic of the Gas Assisted Gravity Drainage (GAGD) Process (Rao et al, 2006)

According to a 2007 Schlumberger market analysis, more than 60% of world's oil and 40% of world's gas reserves are held in carbonate reservoirs. Most of the remaining world hydrocarbon reservoirs are in carbonate reservoirs (Manrique et al, 2006) and thus this project is undertaken to study the application of GAGD process in carbonate reservoirs.

1.1 Research Objectives

1. To visually demonstrate the GAGD process in a glass model using carbonate material as the porous medium for the model.
2. Investigate the effects of grain size on the overall recovery by using different grain sizes of carbonate material used for the packing of the visual model. Initial run for the experiment uses grain size of 300-425 μm particles with a 2" layer of larger sized particles (600 μm) near the horizontal well to restrict entrance of carbonate material thru

the horizontal well pores. Varying sized particles are to be used to compare the effect of grain size on recovery rate.

3. Examine the effect of type of injection gas on overall recovery by varying the injection gas used for the model. Prior physical model studies done by Ruiz in 2006 suggests a higher recovery while using CO_2 gas as the injection gas. This phenomenon is primarily due to the solubility of CO_2 in oil which causes swelling effect and a reduction in viscosity of oil which eventually leads to higher recovery (Jarrell et al, 2002).
4. Investigate the effect of injection rate on overall recovery and breakthrough time. This is hypothesized to be an important parameter as recovery in carbonate reservoirs is very dependent on heterogeneity, oil quality, drive mechanism and reservoir management and EOR processes are effective in fractured carbonate reservoirs (Adibhtla et al, 2006). A high injection rate can create fracture type model in the model and thus would be important to see the dependence of recovery rate due to the gas injection rate.
5. Compare the results for the oil recovery from GAGD in carbonate reservoirs with prior studies using different porous materials such as sandstone, glass beads, ceramics porous media, sintered glass beads. This would allow for comparisons in techniques and the overall results of the process and can be used in the future for field applications or simulation based applications.

2. THEORY AND LITERATURE REVIEW

2.1 Enhanced Oil Recovery (EOR) Process

Tertiary production from a reservoir following the completion of primary and secondary recovery is commonly defined as Enhanced Oil Recovery (EOR). Primary recovery is driven by the pressure difference between the reservoir and production well pressure, generally referred to as the "natural drive" of the reservoir. Once the natural drive of the reservoir weakens and is no longer effective, fluids such as water generally, are injected in to the reservoir to increase reservoir pressure and hence is defined as secondary production (Muskat, 1949). Typically, oil recoveries at the end of both primary and secondary drive are in the range of 20-40 percent of the original oil in place (OOIP), with a very few exceptions (Stalkup, 1984). According to the US Department of Energy (DOE) and the National Energy Technology Laboratory (NETL) estimates close to 374 billion barrels of oil remains in ground after the primary and secondary recovery process is completed in the United States as shown in Figure 2.1 (Kuuskraa et al, 2006). Based on the 2014 EOR survey from the Oil & Gas Journal, there were 109 miscible CO_2 projects and 48 steam injection projects currently ongoing. Also the industry injects about 3.5 billion cubic feet per day of natural and industrial CO_2 to produce 300,000 bbl/day of oil via EOR methods (PennEnergy EOR Survey, 2014). This makes the need for an innovative and well developed Enhanced Oil Recovery process a vital step in unlocking the nation's locked up oil reserves.

EOR process causes physical, chemical, compositional and thermal changes to the reservoir rocks and fluids. The overall recovery efficiency (E_R) is dependent on two sweep

efficiency components, namely the Displacement Sweep Efficiency (E_D) and the Volumetric Sweep Efficiency (E_V). So, $E_R = E_D \times E_V$. These 2 fundamental efficiency factors are vital for a

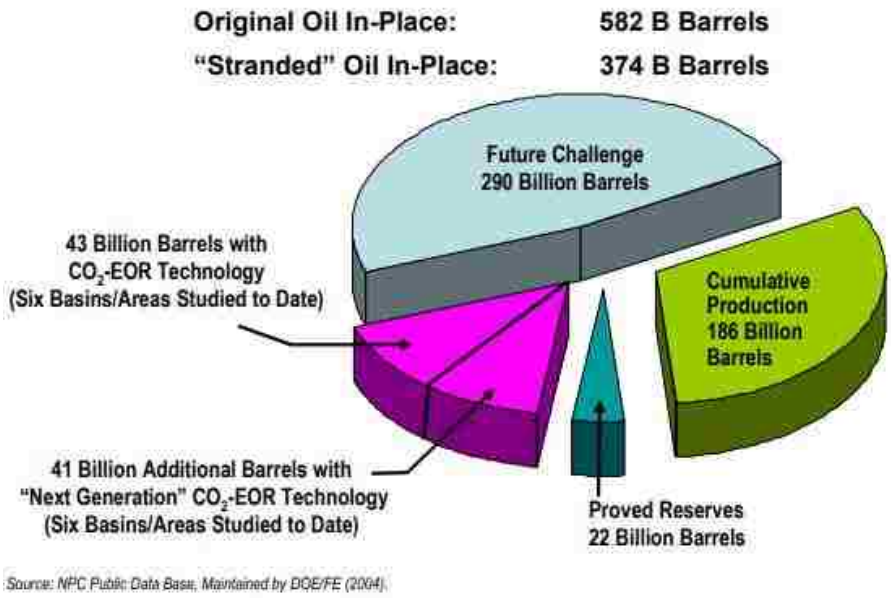

Figure 2.1. Breakdown of US discovered and future production and the estimated "stranded" oil to be recovered through EOR Methods as referenced in Kuuskraa et al, 2006

successful EOR process, an improved mobility ratio for higher volumetric sweep efficiency and an improved capillary number for higher microscopic displacement efficiency. Several existing and currently practiced EOR methods take advantage of one or partially both of these phenomenon to achieve the highest recovery. Most common methods include miscible gas injection (generally CO_2, N_2, and inert gas), chemical flooding, thermal injection, or microbial EOR. Alternatives like the Water Alternating Gas (WAG) process proposed by Caudle and Dyes (1958) takes advantage of a higher volumetric sweep efficiency however, has limitations due to the natural separation of water, oil and gas due to the density differences. Rao (2001) reported

the field application of WAG process yields about 5-10% OOIP. Previous studies have led to the development and optimization of the Gas Assisted Gravity Drainage (GAGD) process. GAGD process is similar to other EOR processes in principle to provide additional pressure to the depleting reservoir pressure from initial production and can thus be applied in either secondary or tertiary stage. GAGD process takes advantage of the natural segregation of fluids in the reservoir through the presence of gravity by injection of gas in the reservoir such that the gas pressure cap will force the oil downwards and thus be captured through the horizontal well. The GAGD process uses CO_2 and N_2 gas as the primary sources of injection gas and its usage achieves both a higher volumetric and microscopic sweep (Rao et al, 2003).

2.2 Previous Related Work

The following section discusses past studies performed using the GAGD technique and summarizes the findings from the past studies. The GAGD process was invented and patented at the Louisiana State University in Baton Rouge, LA (Rao, US Patent 8,215,392). GAGD process has been shown to work in both secondary and tertiary recovery processes (Mahmoud, 2006). GAGD lab based experiments were investigated at LSU beginning 2000 under a federal grant from the Department of Energy. Several technical reports and a final technical report for the research work was submitted to the DOE (Rao et al, 2006). Some of the major previous experimental work is summarized below.

Sharma (2005) studied a water-wet physical model to investigate the effect of different groups of dimensionless numbers such as Bond Number (N_B), Capillary number (N_C), and Gravity Number (N_G) on GAGD performance. He also studied the impact of using different types of gas for injection, namely N_2 and CO_2 and concluded that the different gas types had no significant impacts on recovery rates when injected at constant pressure in immiscible mode.

Further, injecting the gas at constant rate to control N_B and N_C it was found that the higher the N_B the higher the oil recovery.

In 2005, Kulkarni had studied the GAGD process in comparison with other common gas injection process such as Water Alternating Gas (WAG) and Continuous Gas Injection (CGI) methods using scaled corefloods. His work shows that the GAGD process outperforms both of the other processes in both secondary and tertiary mode. Furthermore, his work using scaled corefloods at close to reservoir type pressures show that injecting gas in miscible mode can recover almost all of the initial oil in place (IOIP). He also found that the recovery rate is higher at higher gravity numbers (N_G).

Another study was conducted to study the GAGD process in an oil-wet reservoir. Ruiz (2006) ran the GAGD experiments in a model with glass beads altered from water-wet to oil-wet and discovered higher recovery for an oil-wet medium. It agrees with intuitive consideration that oil-wet medium allows oil to be drained as a continuous film as it drains from the model through the horizontal well. His study also examined the effects of increasing grain size of the porous medium which increased the overall recovery as higher sized grains also increases porosity and permeability. His study also verified the phenomenon studied by Sharma regarding higher recovery from constant injection pressure experiments rather than constant injection rate.

Also, in 2006 Mahmoud studied GAGD process using glass model for secondary and tertiary recovery mode. He also examined that the injection depth does not have a significant influence on the recovery rates as long as there is a communication between reservoir layers. His experiments also showed a higher recovery in fractured porous media versus a homogenous porous media and also found the process to be viable for high viscosity oils. Mahmoud states three mechanisms responsible for the high oil recovery rate through his experiments (as high as

83% IOIP): Darcy-type displacement until gas breakthrough, gravity drainage following breakthrough, and film drainage in the gas invaded zones.

Similar experimental work was done for fractured porous media by Maroufi et al, (2013) where they utilized a cylindrical geometry of unconsolidated packed models. The main parameters studied were the extent of the matrix permeability, physical properties of oil, and the withdrawal rate. They used a controlled gravity drainage and compared the findings with free fall gravity drainage for 15 different test runs. It was found that the decreasing matrix permeability reduced the ultimate recovery significantly whereas the increase in oil properties such as viscosity or density leads to a higher ultimate oil recovery.

The experimental work conducted thus far has focused on the mechanisms of the GAGD process and optimization of the variables of the process. To the best of author's knowledge there hasn't been any experimental work conducted on GAGD process performance in carbonate reservoirs at the beginning of this study. Due to the vast amount of hydrocarbon reserves in carbonate formations, this study will provide insights to GAGD performance in carbonate geology.

2.3 Forces in Oil Reservoirs: Gravity, Capillary, and Viscous Forces

A reservoir with oil, water, and gas presence is impacted by naturally occurring forces acting upon the fluid flow through the porous media within a reservoir: gravitational force, capillary action, and viscosity. The presence of gravity is what results in the separation of the gas, oil, and water zones within a reservoir based on density of fluids and leads to gravity drainage, the self-propulsion of oil in the reservoir rock (Lewis, 1942). The GAGD process works in conjunction with the natural gravitational forces and takes advantage of the natural

phenomenon in reservoirs to push more oil downwards by injection of gas. Typically, oil drains from the pores and flows down dip to the wells. Solution gas drive is responsible for the early part of primary production, yet gravity drainage is evident at the lower part of the reservoir. As the pressure depletes, even other parts of the reservoir see gravity drainage (Terwilliger et al, 1951).

Within a reservoir rock, the fluids distribution for oil, gas, and water is maintained by the wetting characteristics and the capillary interaction of the fluids. The typical reservoir contains an oil-water and gas-oil interface where the interface consists of many menisci, and the capillary forces are relevant at the pore scale as shown in Figure 2.2 along with the other forces that impact displacement of fluids. In a porous medium, like a reservoir, capillary forces have a special importance and the capillary pressure, or the difference between the pressures at the interface of a non-wetting phase with a wetting phase is defined by the Young-Laplace law (Lovoll et al, 2005).

$p_c = p_{nw} - p_w = \gamma \left(\frac{1}{R_1} + \frac{1}{R_2}\right)$ where,

γ = surface tension between the fluids,

R_1 and R_2 is the principal radius of the interface.

Saffman and Taylor (1958) studied the displacement of a fluid by another in a Hele-Shaw cell and showed how the interface stability is impacted by the viscous forces of the fluid. However, in a porous medium the capillary fluctuations at a pore scale and the fluctuating viscous forces can act to stabilize or de-stabilize the displacement front. Therefore, the displacement for drainage in a 2-D porous media depends on the relative magnitude of viscous

forces and gravity, and also their relative magnitude with respect to the heterogeneous capillary forces (Lovoll et al, 2005).

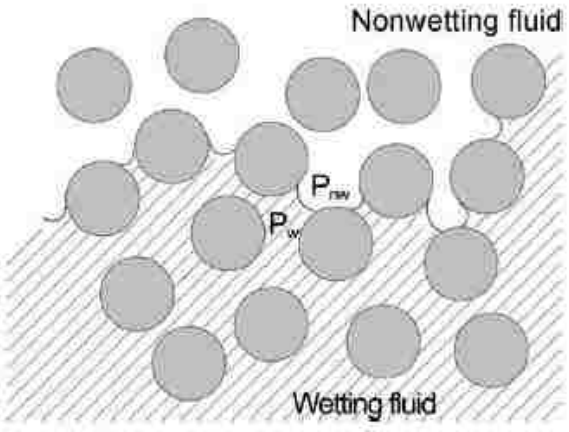

Figure 2.2. Laplace law explains the difference between the pressure in non-wetting and wetting fluids. Capillary action acts against displacement during drainage and thus invasion of larger pore space is easier (Lovoll et al, 2005).

Hence, several past studies with physical models for the GAGD process have utilized a set of dimensionless numbers to understand the influence of different forces during the gravity drainage process. The dimensionless numbers also allows for scaling the lab scale models to field scale and the theory was first introduced by the Buckingham's pi theorem (Geerstma et al, 1956). Dimensionless Gravity number which is essentially a ratio of the gravity force and viscous forces along with dimensionless time are two important set of dimensionless variables shown below (Sharma, 2005).

Gravity Number (N_G): $$N_G = \frac{\Delta\rho g/g_c \left(\frac{K}{\emptyset}\right)}{\mu_0 v_d}$$ where,

$\Delta\rho$ is the fluid density difference,

g is the Newtonian gravity acceleration,

g_c is the gravity acceleration conversion factor,

K is the absolute permeability,

ϕ is the porosity,

μ_0 is the viscosity of the displacing phase,

v_d is the velocity of the displacing phase

Similarly, dimensionless time is defined as shown below (Miguel et al, 2004).

Dimensionless time, $t_D = \frac{KK_{ro}^{o}\Delta\rho g/g_c}{h\emptyset\mu(1-S_{or}-S_{wi})}t$ where,

K_{ro}^{o} is the end-point relative oil permeability,

g is the Newtonian gravity acceleration,

g_c is the gravity acceleration conversion factor,

h is the height of the porous media,

S_{or} is the residual oil saturation,

S_{wi} is the initial water saturation

2.4 Sandstone and Carbonate Lithology

Carbonates are sedimentary rocks that are chemically precipitated in marine environments and are generally of biological origin. They consist mostly of calcium carbonate and go through different geological processes of burial and lithification than sandstones. Carbonates that have undergone burial diagenesis typically form the sedimentary rocks in subsurface processes. Though there are several varieties of carbonates, they are typically made of calcite that precipitates out of shallow marine waters. Most carbonates show signs of multi-diagenetic events, such that they begin with preliminary cementation in the marine environments

and then with different intensity go through the shallow and deep-burial stages (Scholle, 1985). In a very basic scenario, micro crystals of calcium carbonate ($CaCO_3$) occur in sea water and gets deposited at the sea bed, where it forms limey mud. Recrystallization of buried $CaCO_3$ forms limestone. It is vital to understand the geochemistry of the reservoir rocks for a successful reservoir development as these events can lead to the explanation and prediction of various rock properties. For rocks within the deep subsurface several geochemical or petrographic techniques like the light microscopy, stable isotope, trace element, fluid inclusion studies, can be utilized to understand the diagenetic history (Morse and Mackenzie, 1990).

Sandstone can be composed of various different particles such as quartz, feldspar, mica, lithic fragments; essentially sand-sized particles of various rocks. As the larger rocks breakdown due to processes such as erosion, weathering, biologic impacts, etc. they can carried by the rivers to form sand bars of a large delta similar to the Mississippi river. There is a wide range of geologic processes that sandstones can go through and especially the sandstone reservoirs containing oil and gas resources. In the *Sandstone Petroleum Reservoirs* (Barwis et al, 1990), authors discuss 22 unique case studies from a variety of depositional settings, tectonic provinces, and diagenetic history and the impact of the reservoir characteristics on the petrophysical properties, reservoir composition and eventually the hydrocarbon production. Along with the sand particles carried by the rivers, groundwater typically carries minerals that gets deposited within the sand grains. Minerals like calcite, quartz, feldspar, hematitie, cements the sand particles together to form sandstone (as summarized by Kelly, no year).

A world map showing the geographical distribution of carbonate reservoirs and siliciclastic reservoirs is shown in Figure 2.3. The map doesn't show a wide gap of geographic representation of petroleum provinces. Fundamentally, carbonate reservoirs differ from

sandstone reservoir rocks in two ways. First, while sandstone rocks are produced from the allochthonous sediments, carbonate rocks are produced from the autochthonous sediments. Second major difference is the greater chemical reactivity of carbonate minerals (Choquette and Pray, 1970; Moore, 2001, as cited in Ehrenberg and Nadeau, 2005). The chemical reactive nature of carbonate minerals has a significant impact for diagenesis and reservoir quality and thus are characterized by early lithification and porosity modification. Carbonate minerals are generally more soluble, which can lead to the buildup of secondary porosity which is more important than in sandstones. The minerals from carbonate reservoirs are generally more oil wet than sandstone reservoirs. Also fractures are more common for carbonate reservoirs. This would lead to believe that differences in fundamental properties between these two types of reservoir rocks exist.

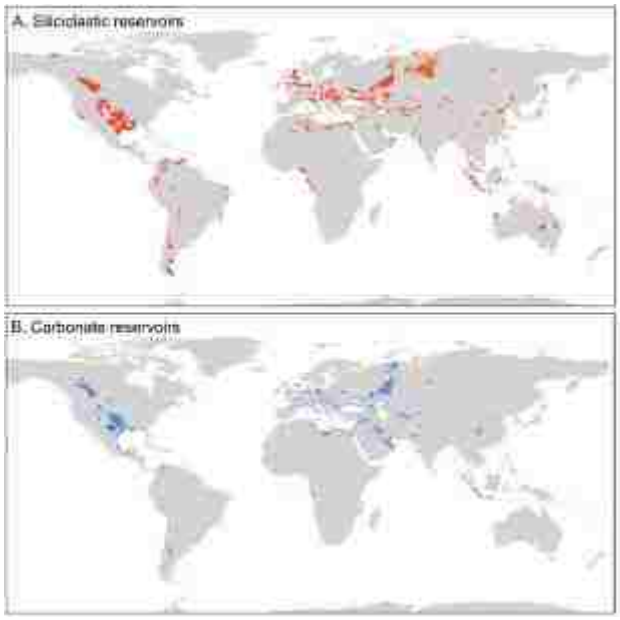

Figure 2.3. Global data for petroleum reservoirs based on their geographical distribution (Ehrenberg and Nadeau, 2004)

Ehrenberg and Nadeau (2005) compiled and compared the reservoir parameters between siliciclastic and carbonate petroleum reservoirs from essentially all producing parts of the world in their work. They compared a total of 30,122 siliciclastic petroleum reservoirs with 10,481

carbonate petroleum reservoirs from all petroleum-producing countries except Canada. Results are shown for Alberta basin in Canada separately. Figure 2.4 below compares the results of the average porosity vs. top depth and also average permeability vs. average porosity relationships from their study. The graph, shown on the left, compares average porosity vs. top depth for sandstone and carbonate global petroleum reservoirs (excluding Canada). The bottom image shows the statistical trends where P90 indicated that 90% of reservoirs have greater porosity than the value, P50 is the median porosity and P10 indicates 10% reservoirs have higher porosity. Some interesting lithology highlighted in the chart for both sandstone and carbonate reservoirs is also noted in the image on the left. For sandstones, the long-dashed green line in the graph is for Tertiary sands of south Louisiana, an example of quartzose sandstone buried at low geothermal gradient. The short-dashed green line on the graph for sandstone is from the offshore mid-Norway of the Middle Jurassic Gam formation, another type of quartzose sandstone buried at moderate geothermal gradient. For the carbonate reservoirs, the dashed green line is representative of the Tertiary and Cretaceous carbonate from south Florida, a shallow-water carbonate lithology buried at low geothermal gradient. The average porosity vs. permeability chart on the right compares the sandstone and carbonate reservoirs from global petroleum reservoirs study conducted by Ehrenberg and Nadeau (2005).

From the relationships shown in Figure 2.4, it is evident that carbonates tend to have lower average and maximum porosity at given depth relative to sandstone reservoirs. The porosity-permeability relationship shows in general slightly higher permeability for carbonates within the 5-20% porosity range however, sandstones have higher permeability at 25-30% porosity. Also, sandstone reservoirs are shown to have higher proportion of high porosity and high permeability relationship. Carbonate reservoirs seem to have higher proportion of high

permeability low porosity reservoirs and this is attributed to the fractures developing in the carbonate reservoirs Ehrenberg and Nadeau, 2005).

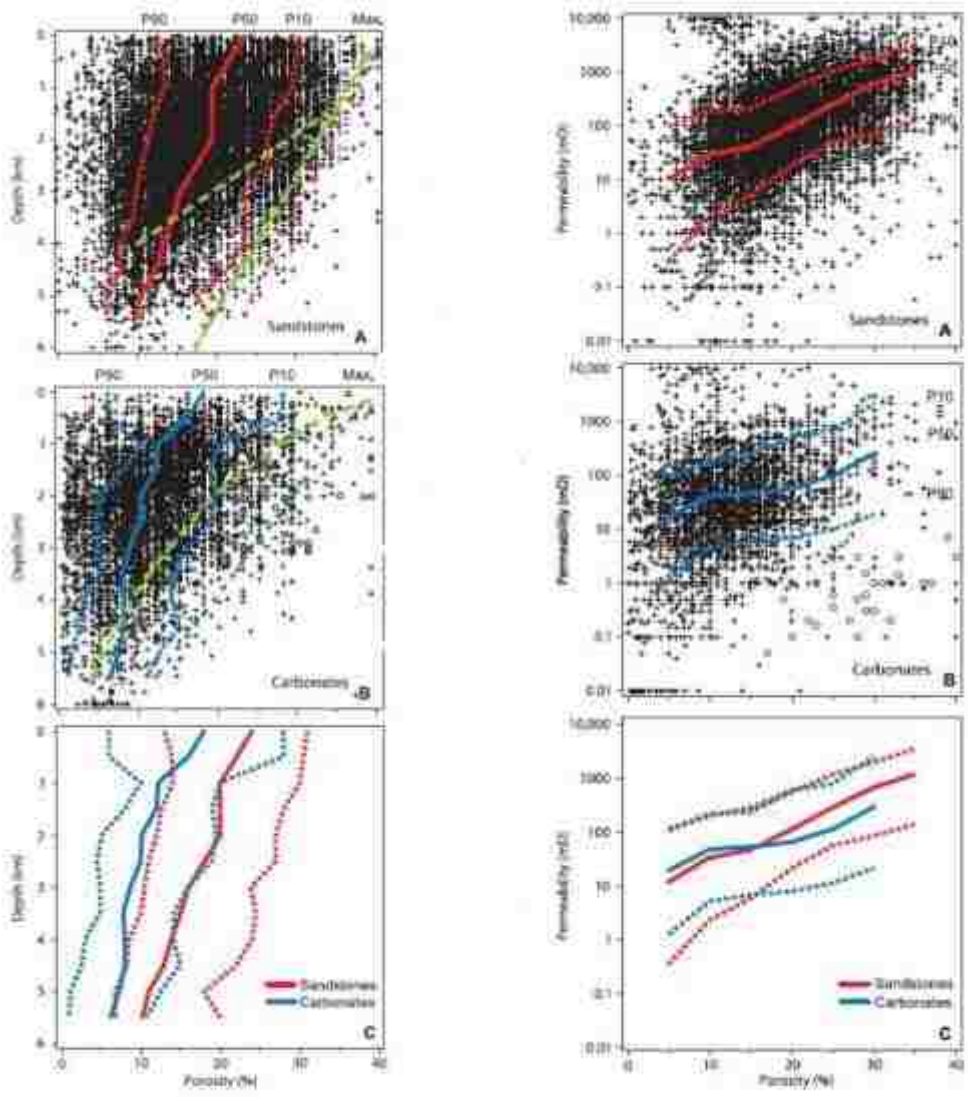

Figure 2.4. Porosity vs. depth and porosity vs. permeability relationships for global petroleum reservoirs (Ehrenberg and Nadeau, 2005)

3. INITIAL MODEL

As carbonate rocks are generally mixed wet or oil wet, the visualization of the flow of the fluids through the model, particularly the flow of oil through the porous media is of high interest for this study. Visuals models were used in past experiments studying the GAGD process in sandstone materials as the porous medium. Past studies built the models in the lab using glass plates and glue. For this study, a tank was ordered from an aquarium store as it could serve the purpose well and also save time in the model building process. One drawback was the tank was designed to be used as a fish tank thus not withholding too much pressure. However, the pressure limits were not provided by the manufacturer.

A model was built and initial water saturation was performed. During this run, a pump was used for injecting water into the fluid. Thus the model was connected to the TELEDYNE ISCO series D pumps from the base of the model to inject water into the model. The outlet for the model was connected to a produced fluid collection cylinder. To ensure gravity stabilized flooding the general rule of thumb used to do the flooding is to inject heavier fluids (water) from bottom to top of the model and vice versa for lighter fluids (oil and gas). Figure 3.1 shows the pump used for injecting fluids from the pump in to the model.

The pumps control unit allows the user to control the flow rate and also enables to program refill time and rate of the fluids in the pump. This system of pump uses gas as a source of pressure to move the fluids across the pump. The pump has two cylinders to allow for continuous injection however, cylinder on the left side of the pump seemed to be malfunctioning as it would not inject at a rate set at the control system. Only one cylinder chamber was used for injection to ensure a proper volume calculation for determining the pore volume of the system. The pump

control system as shown in Figure 3.2 was turned to an injection rate of 1 mL/min and changed to 3 mL/min as more fluid was injected into the model.

Figure 3.1. Teledyne ISCO Series D Pump used initially for fluid injection

Figure 3.2. Pump Controls for the Series D Pump

Set of images shown below in Figure 3.3 show the progression of the water front through the model. The top outlet for the model is kept open while the water is injected from the bottom. The side outlet at the bottom opposite from which the water is inject is kept shut using the valve installed on the tubing.

Figure 3.3. Water front propagation moving through the model upon initial water saturation run

The initial water injection through the model allowed the determination of the pososity of the model to be 39.4%. The total volume of water inside the model was measured at 1175.58 mL while the bulk volume for the model is measured to be 2980.8 cm^3. The fluid volume inside the

model was calculated by eliminating all the dead volume in the tubes connecting the model and the pumps injecting the fluid.

Since, $\phi = \frac{V_p}{V_b}$, where ϕ is porosity and V_p and V_b are pore volume and bulk volume respectively, the porosity value yields a 39.4% porosity in the model. After measuring the porosity for the model, the next step was to measure permeability for the model. While running the permeability tests, model reached a pressure of 10 psi at a flow rate of 6ml/min near the inlet of the water through the horizontal well which caused the model to break. This was a huge learning lesson for the project as careful consideration needs to be given on the amount of pressure applied to the model throughout the project. A new model was then built as described in the next section as the experimentation setup was moved to the new lab in the renovated Patrick F Taylor hall. The following Figure 3.4 shows the result of the crack that developed in the model once it reached a pressure of 10 psi.

Figure 3.4. Cracked model due to the increased pressure

4. APPARATUS AND EXPERIMENTAL PROCEDURES

4.1 Experimental Setup

The experiments were conducted to visualize the gas assisted gravity drainage (GAGD) process of oil recovery by gas injection, using both CO_2 and N_2 gas in carbonate rocks. As the experiments were conducted in a glass tank, initial learning curve was to understand the pressure ratings that the model can withstand without breaking. As described in the above section of initially damaged model attempt, it was soon realized that the model can withstand extremely low pressures before failing (< ~10psi) and some of the procedures below were since modified to allow for minimal pressure to the model. The model setup while running the GAGD process can be seen in Figure 4.1 below. The effects of grain size, injection rate, and injection gas were tested. The experimental materials and procedure used for the GAGD process is described in this chapter below.

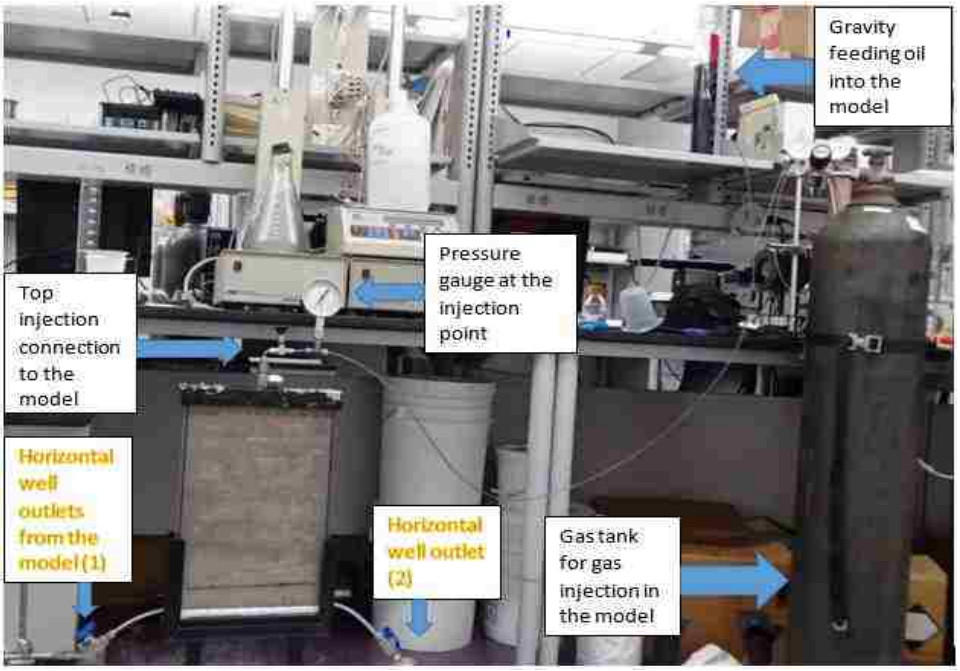

Figure 0.1. Experimental Setup using gravity feed for Water & Oil

4.2 Experimental Materials

To study the GAGD process in carbonate reservoirs similar materials and procedures have been used as in past experiments studying the GAGD procedure. A glass model is used to visualize the process, the model used is shown in Figure 4.2. Below is a list of materials used for the experiments.

- Glass model with outside dimensions of 12” x 2” x 20” was supplied from Planet Aquarium in Arlington, TX. See Figure 4.2.
- Indiana Limestone in chunks were supplied from Kocurec Industries in Caldwell, TX. See Figure 4.3. The chunks of limestone were further crushed and sieved into the desired particle sizes for the experiment. An XRD analysis of the limestone material shows the below composition for the material. The XRD report analysis is attached in Appendix B.

Table 0.1. Composition of the Limestone material from a XRD analysis

Material	Chemical Formula	Composition
Calcium Carbonate	$CaCO_3$	98%
Silicon Dioxide	SiO_2	2%

- Mortar and pestle was used to crush the chunks to be used for packing the model. See Figure 4.4.
- Ro-Tap mechanical Sieve shaker was used to sieve the crushed limestone material. The sieve shaker was manufactured by W.S. Tyler, see Figure 4.5.
- Mechanically precise drill was used for perforating the horizontal well tubing used in the model from the Advanced Manufacturing and Machining Facility at LSU. See Figure 4.6.
- A vacuum pump was used to remove trapped air from the model. See Figure 4.7.

- Distilled water from the lab
- n-Decane, used as oil for the experiment, with 99+% purity was purchased from Fischer Scientific Company.
- Sudan black B dye from Fisher Scientific was used to differentiate Decane in the model
- Hexion EPON Resin 828 was used along with EPIKURE 3125 Curing agent, both supplied by Miller –Stephenson Chemical Company. The industrial strength epoxy has a rated adhesive property shear strength of up to 6,000 psi along with resistance to a broad range of chemicals including fuels and solvents. These set of properties made this an attractive choice of epoxy to be used for our purposes. A technical data sheet for the epoxy has been attached in Appendix C.
- CO_2 and N_2 pressurized gas cylinders supplied by AirGas were used for gas injection
- Pressure gauges are used to measure inlet or outlet pressure as needed.
- Cole Palmer flowmeter (Model # PMR 1-010345) was used for controlling flowrate for gas injection.
- A frame was constructed at the LSU mechanical shop to hold the model in place.

Figure 0.2. Glass model used for the experiments

Figure 0.3. Chunks of Indiana Limestone rock as received from the supplier

[redacted]

[redacted]

Figure 0.7. Vacuum pump used to remove trapped air from the model

4.3 Preparation of the Glass Model for GAGD Runs

As described in the materials section above and shown in Figure 4.2, a total of 3 different glass tanks with approximate dimensions of 12” x 2” x 20” was ordered from Planet Aquarium in Arlington, TX. The tank was delivered with 2 holes of ¼” diameter drilled just above the base of the tank to allow the placement of the tubing to be used as a horizontal well for the experiments. The tank was further modified in the following steps to prepare it for running the GAGD procedure.

1. Plastic tubing of ¼” diameter is used as the horizontal well that is placed at the bottom of the model. The tube has holes drilled throughout the top end of the pipe to allow fluid flow. The length of the tube spans across the glass model. The holes are drilled to ensure that the carbonate material right above the tubing is larger than the hole size to ensure that they don’t pass through the well or block the holes. Thus, the holes are drilled carefully with a 1/64” (~400 μm) drill from the Advanced Manufacturing and Machining facility (AMMF) at LSU. It is important that care is taken to keep the holes in a consistently spaced manner. A grid type-pattern was made with three rows of holes on the front end of the pipe. Figure 4.8 shows the process and the equipment used.

2. Since the horizontal tubing holes are drilled slightly above the base of the tank for structural integrity, a spacer was used at the bottom of the model of ¼" height to eliminate any "dead space" below the horizontal well. Additionally, epoxy was injected surrounding the spacer to ensure its stability and remove the dead space not removed by the spacer. Hexion's Epon Resin 828 was used as epoxy with a curing agent. Once the spacer was allowed to set in along with the epoxy giving a firm base for the horizontal tubing, the tubing was placed in the model.
3. Once the horizontal well was placed and sealed using the epoxy and resin mixture, the model was packed with carbonate material of appropriate size. The carbonate rocks were crushed using mortar and pestle and sieved using the mechanical sieve shaker to obtain the particle size to fill the models. 2 models are used for the experiments with the particle size distribution as shown in table 4.2 below. While packing the model, the materials are squeezed together various times to ensure a tightly packed model. The 2" column with larger grain sizes used in Model # 1 was to ensure that the particles did not escape from the horizontal well or plug the horizontal well tubing. The packing is shown in the Figure 4.9 below.

Table 0.2. Particle Size Distribution for the models used for experimentation

Model #	Model Dimensions (L x W x H) (O.D.)	Particle Size (first 2" from the bottom)	Particle Size (remainder of the model)
0 (Damaged)	11.5" x 1.7" x 19.5"	600 μm	300-425 μm
1	10.75" x 1.7" x 19.5"	600 μm	300-425 μm
2	11.5" x 1.5" x 19.5"	600 μm	600 μm

Figure 0.9. Placement of a 2" layer of higher sized carbonate grains (600 μm) in the model

4. The crushed composite limestone was used to measure the density of the material and to precisely determine the requirements for the model. As such, the material requirements were calculated with the following density calculations for the model. Using the volume of the model at 319.6 in^3 = 5237 cm^3, and grain density of 1.25g/cc.

$$5237\ cm^3 * \frac{1.25\ g}{cm^3} = 6547g * 1.3\ (S.F) = 8511g * \frac{2.2\ lb}{1000\ g} = 18.7\ lbs$$

It was determined that almost 19 lbs of limestone material may be required to fill the entire model with the crushed limestone rock.

5. The sieving process is done using a mechanical sieving machine as illustrated in Figure 4.5. A small sample is placed in the top most sieve and the machine is run in segments of 2-3 minutes for a total sieving time of about 10 minutes per sample. This is the ASTM recommended method for getting a fine particle distribution of the appropriate sized particles. Sieved materials are intended to form the layers of different sized crushed carbonate with the larger grain size material at the bottom to allow a sand packing effect near the horizontal well at the bottom of the tank. This should also allow

the crushed rocks of larger size to restrict passing of the smaller sized grains through the horizontal well while allowing the fluids to pass through.

6. Once the model was fully packed to the top edge, another spacer (similar to the one used at the base below the horizontal well) was placed to seal the top edge with a ¼" threaded hole opening for the fluid movements in and out of the model. The ¼" threaded hole was made using a NTP drill using a taper pipe reamer type drill bit. The spacer was sealed with an epoxy and resin mixture.
7. NUPRO SS-4TF2 60 μm filter fitting is fitted at the top end of the model as the gas inlet valve. The model is thoroughly glued together from all edges after this step to ensure a full leakage proof model.
8. Connection tubing and valves are used at the 2 openings at the bottom end of the model and 1 opening at the top end of the model. This can be seen in Figure 4.1 above.
9. The next step before running the model with the GAGD procedure was to vacuum the model for any trapped air inside the model. As shown in Figure 4.10 below, the model was hooked up with a vacuum pump and ran for almost 30 minutes. If the model holds vacuum, one can validate there are no leaks in the model.
10. Additionally, a stand was fabricated at the Advanced Manufacturing and Machining Facility (AMMF) to hold and place the model while running the tests. Once the model is fully sealed it is ready to begin the initial water saturation run followed by the GAGD procedure, described in the following section.

Figure 0.10. Vacuum Pump applied to the model prior to GAGD runs

4.4 Experimental Procedure

The experimental procedure described below was used for the different experiments conducted for secondary mode gravity-stable gas injection. A summary of the experiments conducted is included in the following section titled “List of experiments conducted.” Some steps were simplified to allow for minimal pressure on the model and to attain largest visibility of fluid flow while keeping the procedure as accurate as possible. Most fluids were gravity fed for injection in to the model, on the other hand gas injection was controlled by valves to the desired injection rate. The experimental procedure followed is listed below in details.

1. Once the model is fully sealed, make connection tubing to imbibe water into the model from the bottom end near the horizontal well. Deionized water is used with a simple hydraulic static head as shown in Figure 4.1. Ensure the top valve is open to allow for air to escape the model and eventually once the model is saturated allowing water to escape

the model from the top. Record the total volume of water inside the model to calculate the pore volume using the formula below.

$$\phi = \frac{V_p}{V_b},$$

Where ϕ is porosity and V_p and V_b are pore volume and bulk volume. Pore volume is the total volume of water inside the model and bulk volume is calculated using the inside dimensions of the model.

2. Once the model is fully saturated with water and the flow inside the model equals the flow out of the model, use a stop watch and a pressure gauge and allow water inside the model to measure the permeability. Calculate the flow rate and using the below formula, calculate the permeability for the model.

$$K = \frac{q\mu L}{A \triangle P}$$

where k is permeability, q is flowrate, μ is the viscosity of water, L is the length of model

3. Once the model is fully saturated with water, begin flooding oil (dyed decane) from the top of the model and ensure both valves at the horizontal well are open to allow water out of the model. Again, the oil is placed above the model and gravity fed into the model. The volume of oil entered through the model is about twice the pore volume, to ensure full saturation of oil. Using material balance, the water remaining in the model is the connate water saturation S_{wi} and the oil in the model is the Initial Oil In Place or IOIP.
4. Now the model is ready for gas flooding. Connect the model from the top with the gas cylinder with a flow control valve and pressure gas connected within the line to allow for desired flow rate and to measure the pressure into the model. Initial tests were performed

to ensure proper model calibration and the volume of oil and water produced from the horizontal well is measured at set frequency.

5. Once the gas breakthrough point is reached, the production starts to taper off. To ensure maximum recovery the model is flooded for several hours beyond the breakthrough point. Generally it was found maximum recovery was reached within 5-7 hours and thus most runs were stopped after 9 hours of gas flooding. The breakthrough points are determined from the pressure data measured every 5 minutes, a sample of the data collected is shown in Appendix A.
6. For the following set of runs with different flow rate, oil is flooded from the bottom of the model to ensure gravity stable injection and the same procedure is followed from Step 4-5 above. Similar measurements are recorded for each run and the data is discussed in the following section.

5. RESULTS AND DISCUSSION

The purpose for this study is to visualize the GAGD process in carbonate rocks using a glass model along with calculating and analyzing the recovery values from the process. The results section presents and summarizes the experimental results obtained from this study. The experiments are designed to visualize the GAGD performance in carbonate rocks as well to determine the impact of injection gas type (Nitrogen or Carbon dioxide), different injection rates, and different grain size packing of carbonate rocks on the overall recovery. The experimental values are also scaled using dimensional time analysis to compare with real field values. The results are for two different models packed with different grain size carbonate materials. Secondary recovery mode was used for oil production for the GAGD experiments performed in this study, it is assumed that the primary depletion drive has been completed. An attempt was made to run the GAGD experiments in tertiary recovery method however, due to the limitations of the equipment it was not feasible. Attempting vertical flooding after secondary recovery removed all the remaining oil from the model and hence horizontal flooding was required. The model needed to be rotated to its side to perform horizontal flooding after secondary recovery. Therefore, tertiary mode recovery was not attempted for this study. The results for both models are shown in the following sections. The set of experiments that were run on the two models are described in Table 5.1 below by the labels and descriptions used in the following part of the results.

Table 0.1. Summary of Experimental Runs with labels and descriptions

Model # 1 (Grain size = 300-425 µm)		**Model # 2 (Grain size = 600 µm)**	
Run #	**Parameters**	**Run #**	**Parameters**
Run N_2.5	N_2 @ 2.5 cc/min	Run 2N_2.5	N_2 @ 2.5 cc/min
Run N_5_1	N_2 @ 5 cc/min_1	Run 2N_5_1	N_2 @ 5 cc/min_1
Run N_5_2	N_2 @ 5 cc/min_2	Run 2N_5_2	N_2 @ 5 cc/min_2
Run N_7.5	N_2 @ 7.5 cc/min	Run 2N_7.5	N_2 @ 7.5 cc/min
Run FG	Free Gravity Drainage	Run 2FG	Free Gravity Drainage
Run C_2.5	CO_2 @ 2.5 cc/min	Run 2C_2.5	CO_2 @ 2.5 cc/min
Run C_5	CO_2 @ 5 cc/min	Run 2C_5	CO_2 @ 5 cc/min
Run C_7.5	CO_2 @ 7.5 cc/min	Run 2C_7.5	CO_2 @ 7.5 cc/min

Initial porosity and absolute permeability were calculated for both models at the beginning of the experiments. In addition to the packing of the models as described in the previous section, the calculated properties for the models are summarized in Table 5.2 below.

Table 0.2. Model Parameters for the GAGD experiments performed

Model #	Model Dimensions (L x W x H)	Grain Size (µm)	Pore Volume (cc)	Porosity (ϕ)	K (mD)	S_{or}	S_{wi}
1	10.75” x 1.7” x 19.5”	300-425	1085	34.2%	1490.28	94.5%	5.5%
2	11.5” x 1.5” x 19.5”	600	1200	40.07%	1920.73	87.5%	12.5%

As seen in table 5.2, the two models were packed with different grain size of carbonate materials which in turn results in larger porosity for the second model packed with larger grain size diameter particles of carbonate rock. Also, the particle grain size affects the effective permeability for the model as calculated from the two models. As permeability is measured using Darcy’s law, the pore volume of the two models varies which creates a pressure difference at

varying flow rates creating a larger permeability for the second model with higher pore volume. The initial oil saturation (S_{oi}) and initial water saturation (S_{wi}) are determined once the model is fully saturated with oil and water.

5.1 Free Gravity Drainage

The base case experiment was run with just gravity force acting on the model by leaving the model open at the top inlet and allowing the system to drain solely with gravitational force. This run is called “Free Gravity Drainage” and is used as a base case to compare the results of the gas injection recovery rates. It also helps quantify the impact of the gravity force on the model and to ensure the presence of capillary pressure in the model similar to a field. The two models used for the experiments are packed with different grain size diameter particles, where model# 1 is packed with particle diameter of 300-425 μm and model# 2 is packed with 600 μm carbonate particles throughout the model. The free gravity drainage for both models is almost identical with about 60% recovery in the first 50 mins of drainage. The results are higher than the previous study from Mahmoud (August 2006) using sand as the packing material where he received a recovery of 43% IOIP. This increase in recovery is expected because of the oil-wet nature of carbonate rocks which forms oil film type drainage which is also visible from the experimental runs. The drainage is visually similar to the following runs as gravity is the dominant force in the initial draining of the model. However, an area of the model remains saturated with oil at the bottom part of the model towards the end of the run as shown in Figure 5.1 below. As the gravity force is unable to overcome the capillary force from the remaining oil in the model, the residual oil remains inside the model. The recovery rates for the two models are shown in Figure 5.2 and the recovery profile from Figure 5.2 shows that the production lasted for a short time and then stopped completely right after breakthrough. Table 5.2 summarizes the

model variables used with the different grain size comparisons for the separate models shown before in Table 4.2.

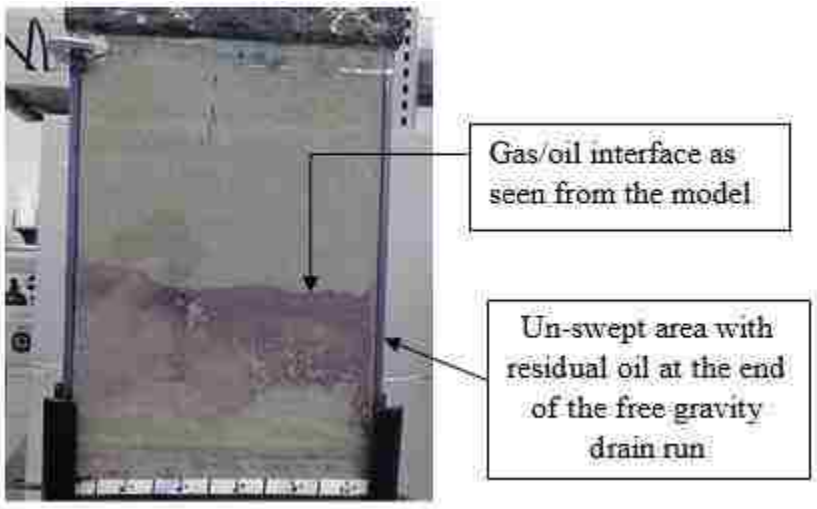

Figure 0.1. Model # 1 at the end of the free gravity drainage

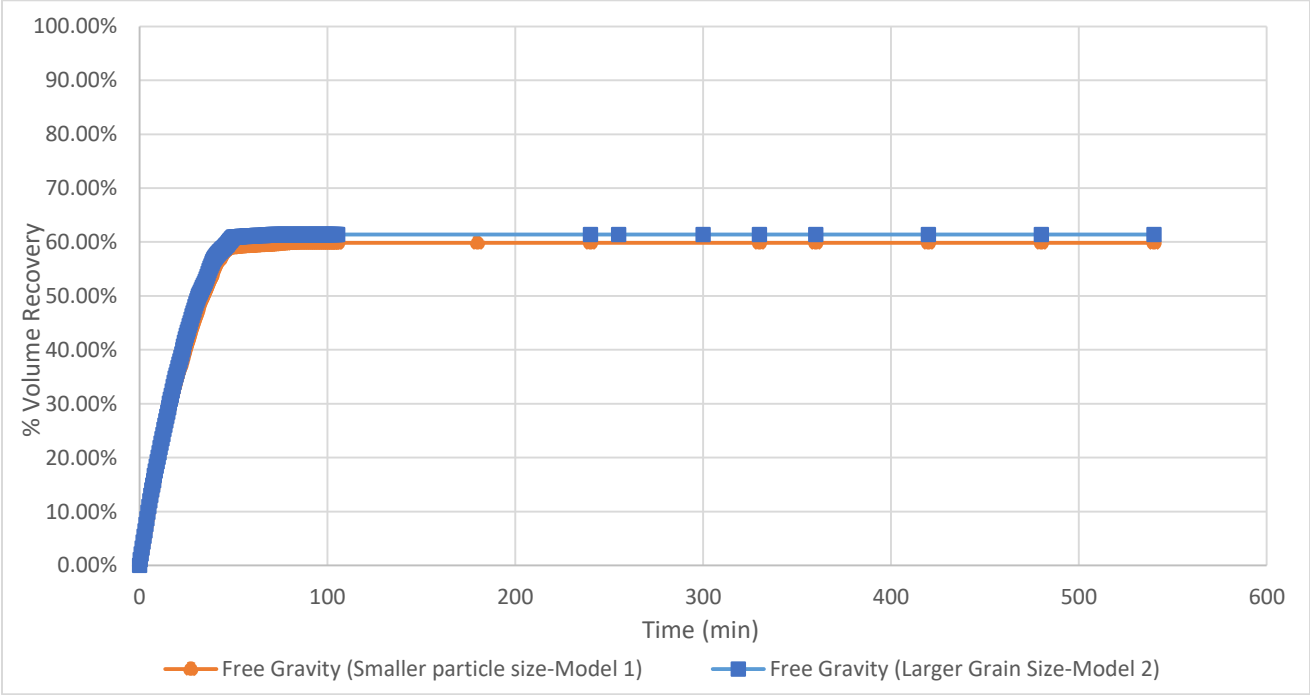

Figure 0.2. Oil Recovery during free gravity drainage

5.2 Effect of Type of Gas Injected

This study tested the effect of the injection gas on the production rate for GAGD on carbonate models. Several past studies conducted on GAGD performance in sandstone material used both nitrogen and carbon dioxide gas as injection gases. To make the comparisons with past studies, the experiments for this study were also conducted using Nitrogen and Carbon dioxide gases for the GAGD runs. The model parameters were similar to as described in Table 5.2 earlier. The pressure at the gas injection point was kept minimal and never went above 0.2 psig to avoid any damage to the glass model. The flow rate was the controlling parameter and were kept uniform throughout the experimental run using a Cole Palmer flowmeter (Model # PMR 1-010345). The production and recovery from the two models at various different injection rates are shown in the charts below (Figures 5.3 to 5.8). The overall production by volume and the production by percentage of oil recovery is summarized in Table 5.3. A propagation front of the gas flood is shown in Figures 5.9 to 5.12, where the visualization of the GAGD process in carbonate rocks can be observed.

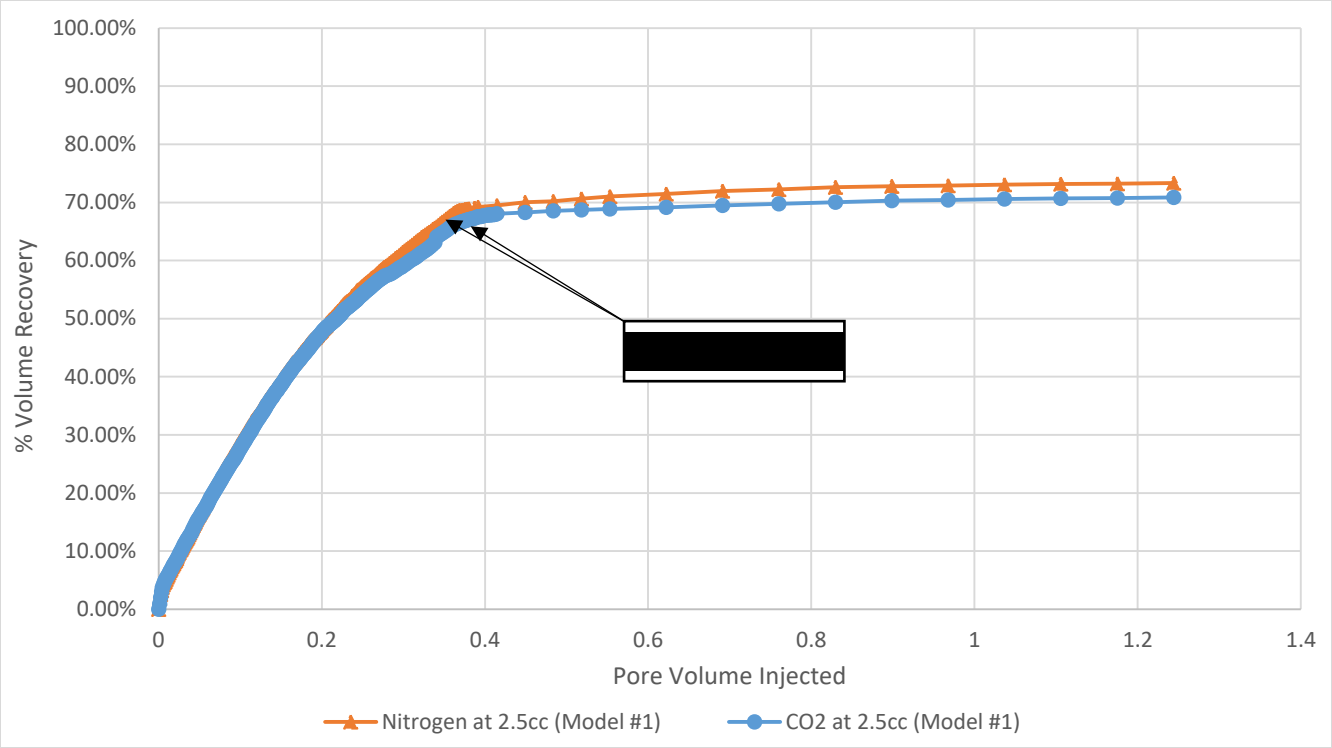

Figure 0.3. Oil Recovery for Model # 1 at 2.5 cc/min with Nitrogen and Carbon dioxide as injected gases

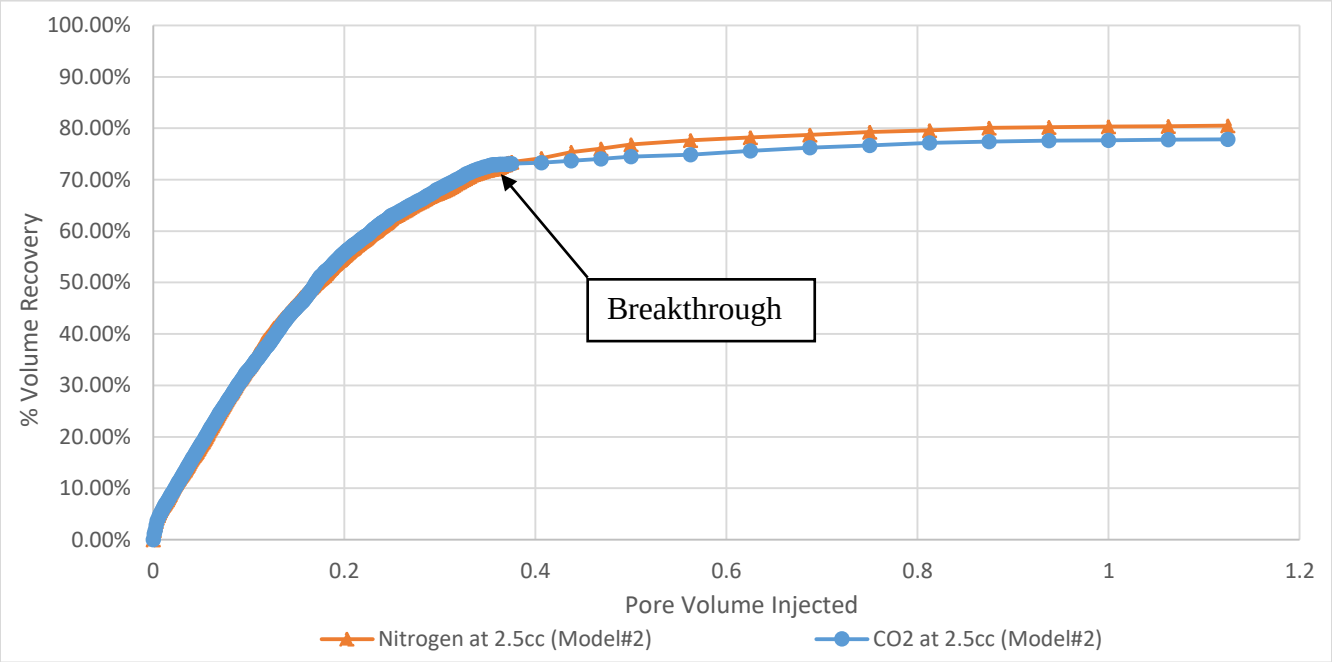

Figure 0.4. Oil Recovery for Model # 2 at 2.5 cc/min with Nitrogen and Carbon dioxide as injected gases

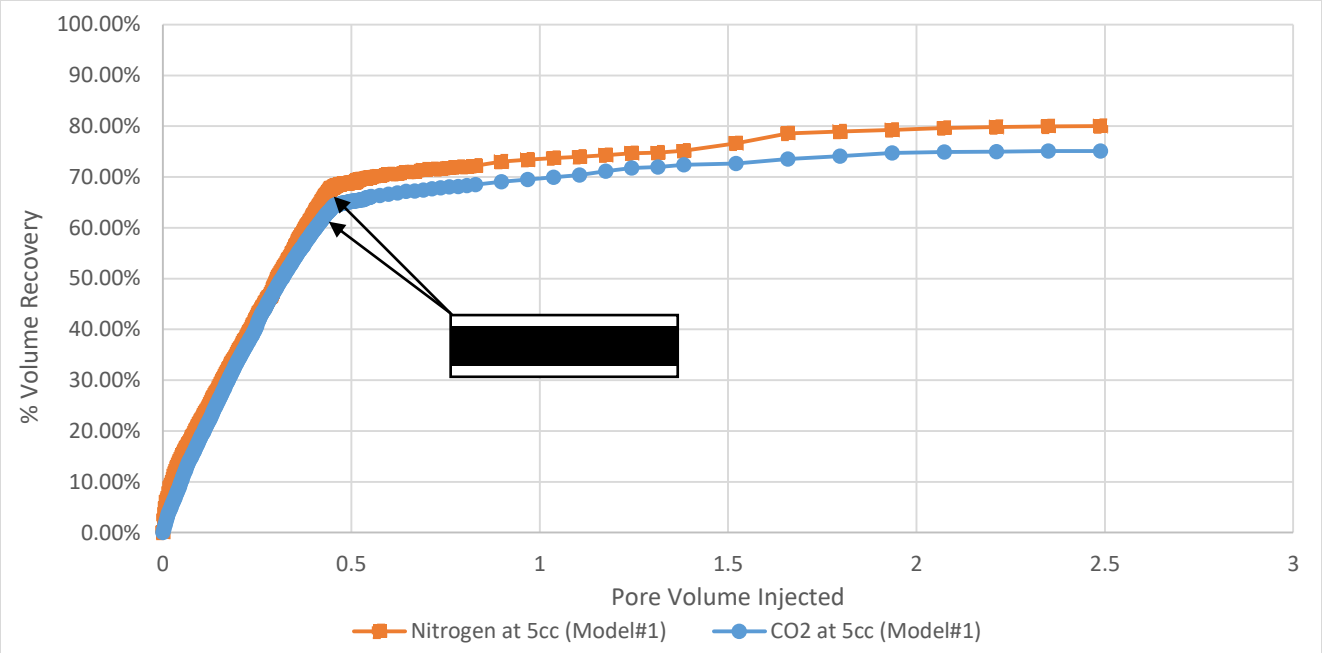

Figure 0.5. Oil Recovery for Model # 1 at 5 cc/min with Nitrogen and Carbon dioxide as injected gases

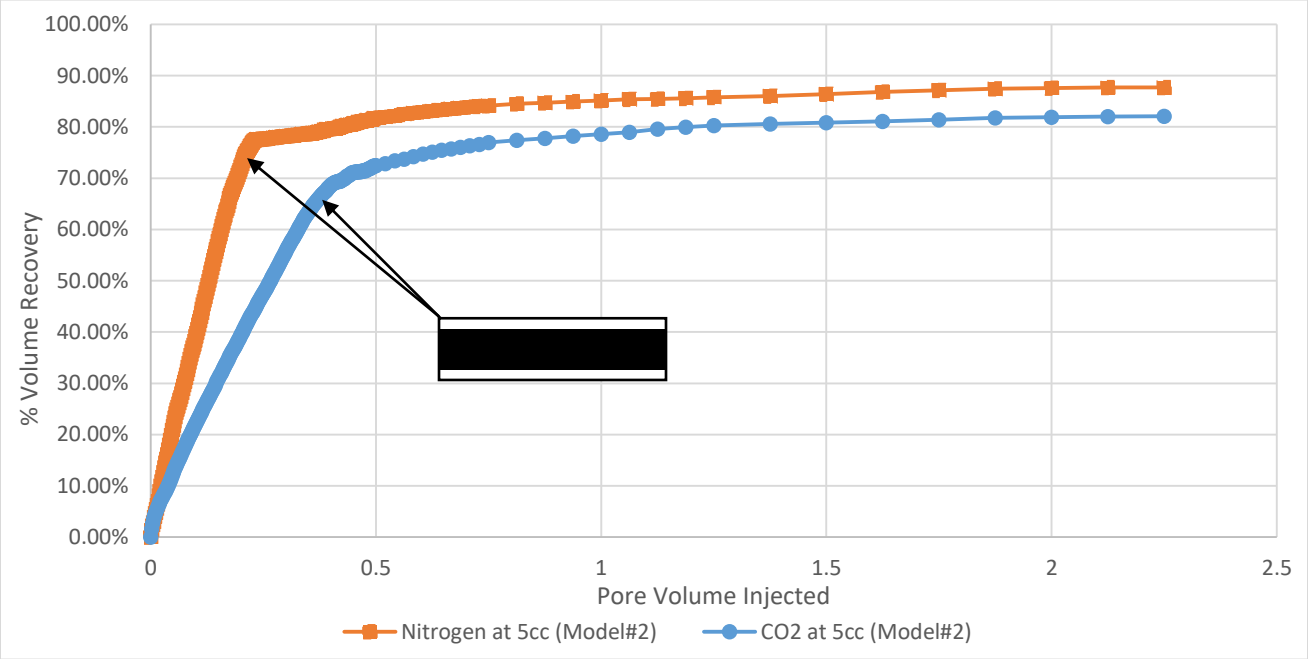

Figure 0.6. Oil Recovery for Model # 2 at 5 cc/min with Nitrogen and Carbon dioxide as injected gases

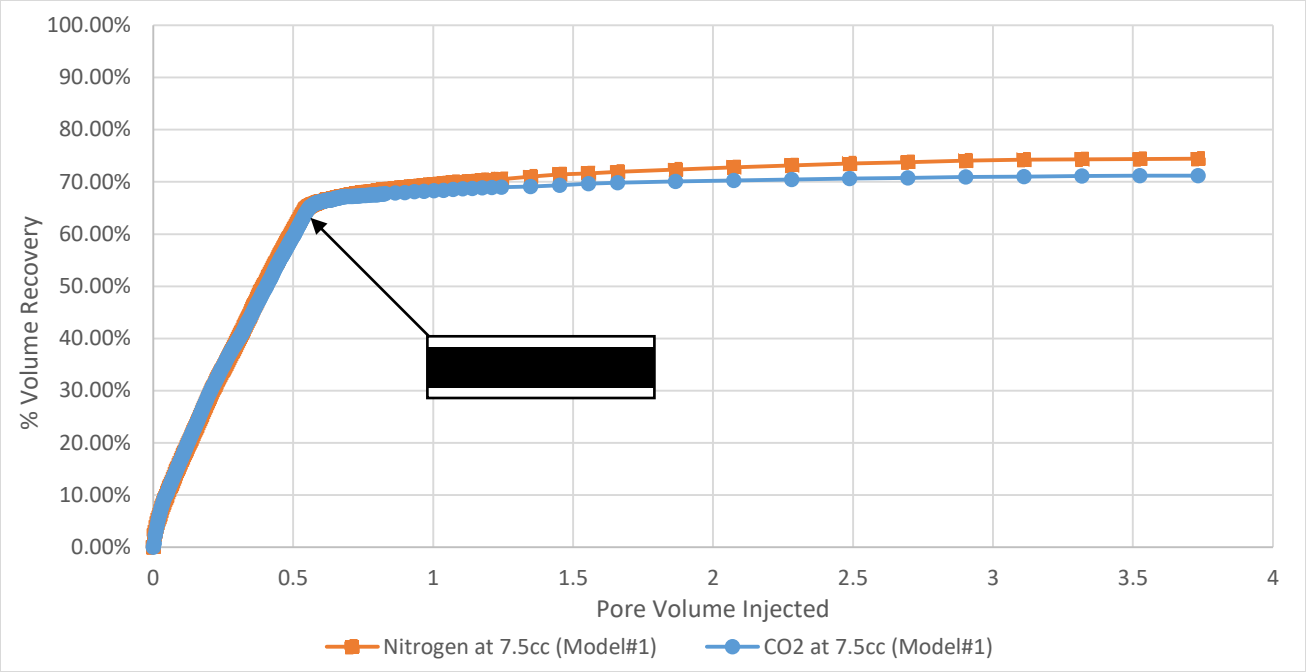

Figure 0.7. Oil Recovery for Model # 1 at 7.5 cc/min with Nitrogen and Carbon dioxide as injected gases

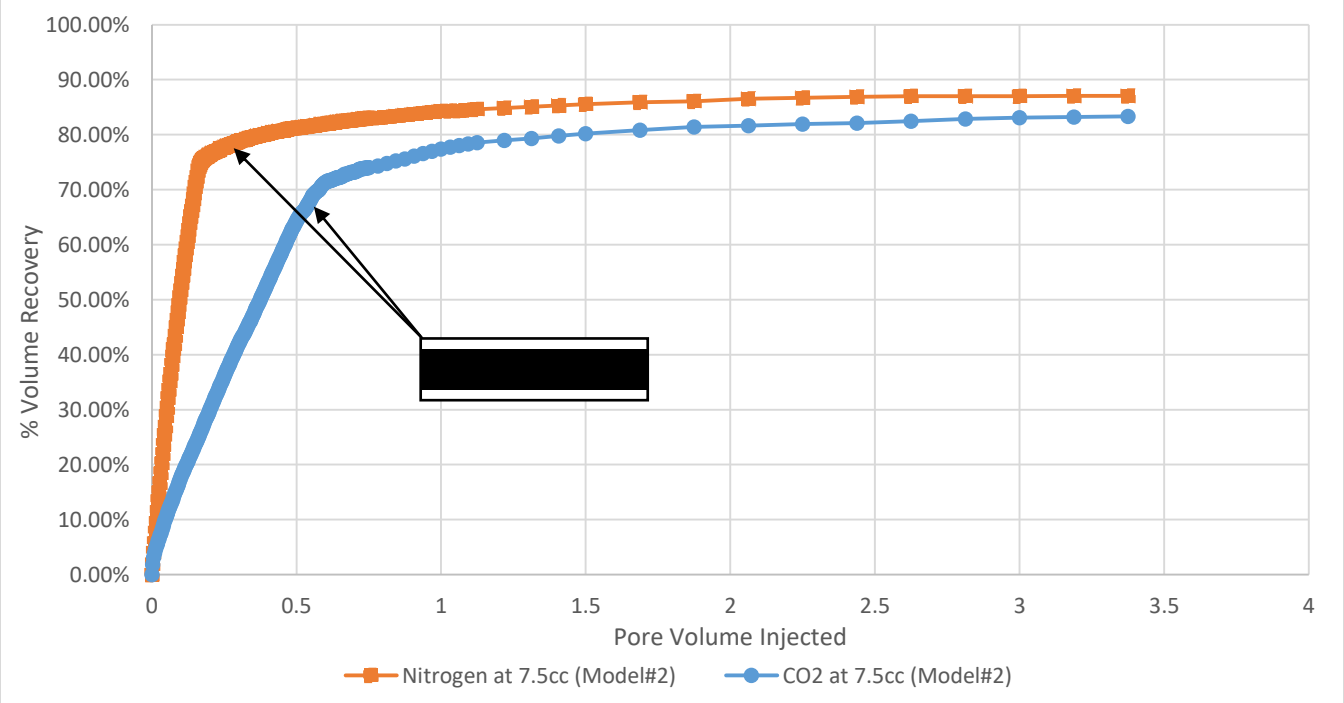

Figure 0.8. Oil Recovery for Model # 2 at 7.5 cc/min with Nitrogen and Carbon dioxide as injected gases

Figure 0.9. Front propagation for N_2 flooding at 5 cc/min for Model # 1 (1 of 2)

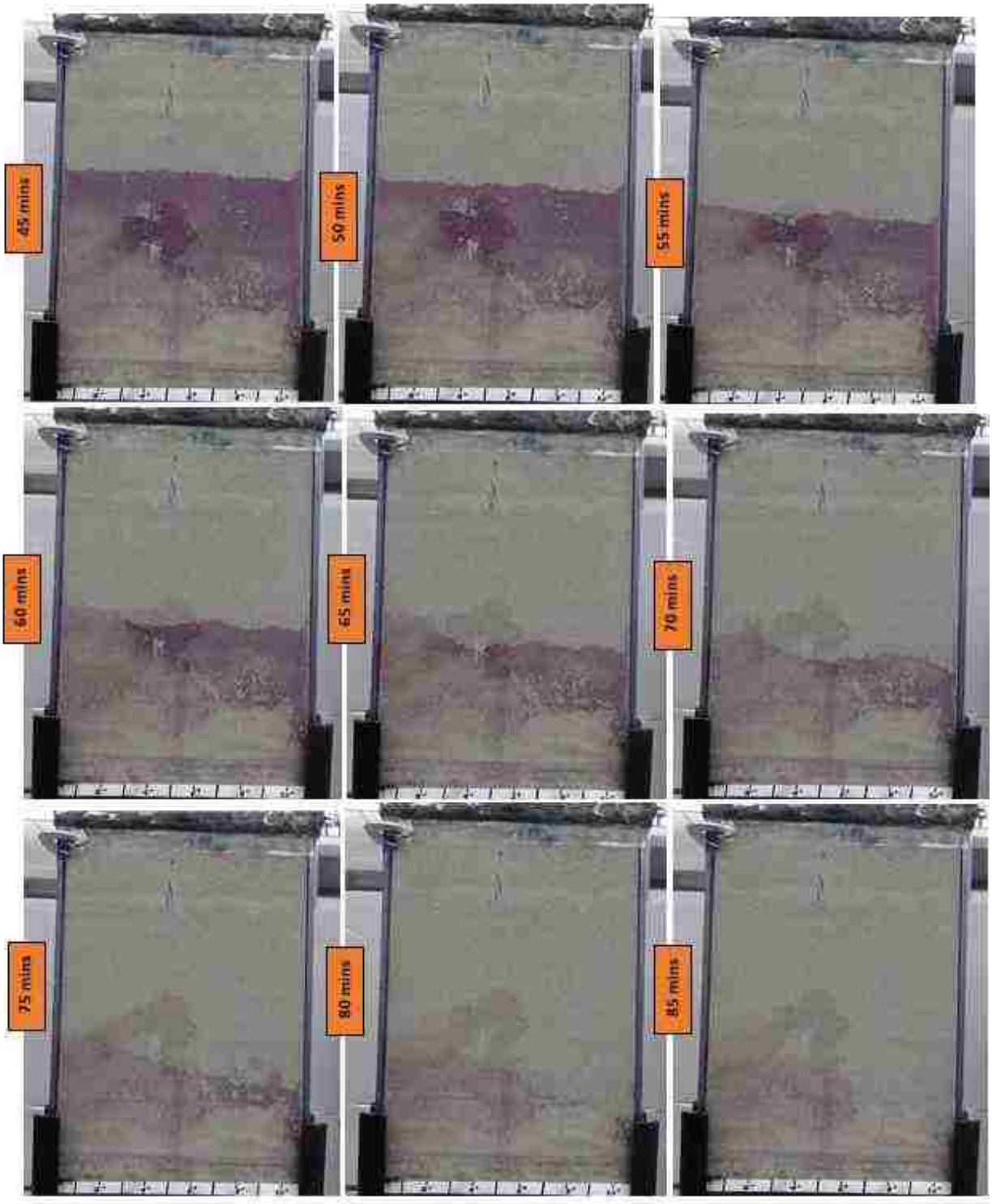

Figure 0.10. Front propagation for N_2 flooding at 5 cc/min for Model # 1 (2 of 2)

Figure 0.11. Front propagation for CO_2 flooding at 5 cc/min for Model # 1 (1 of 2)

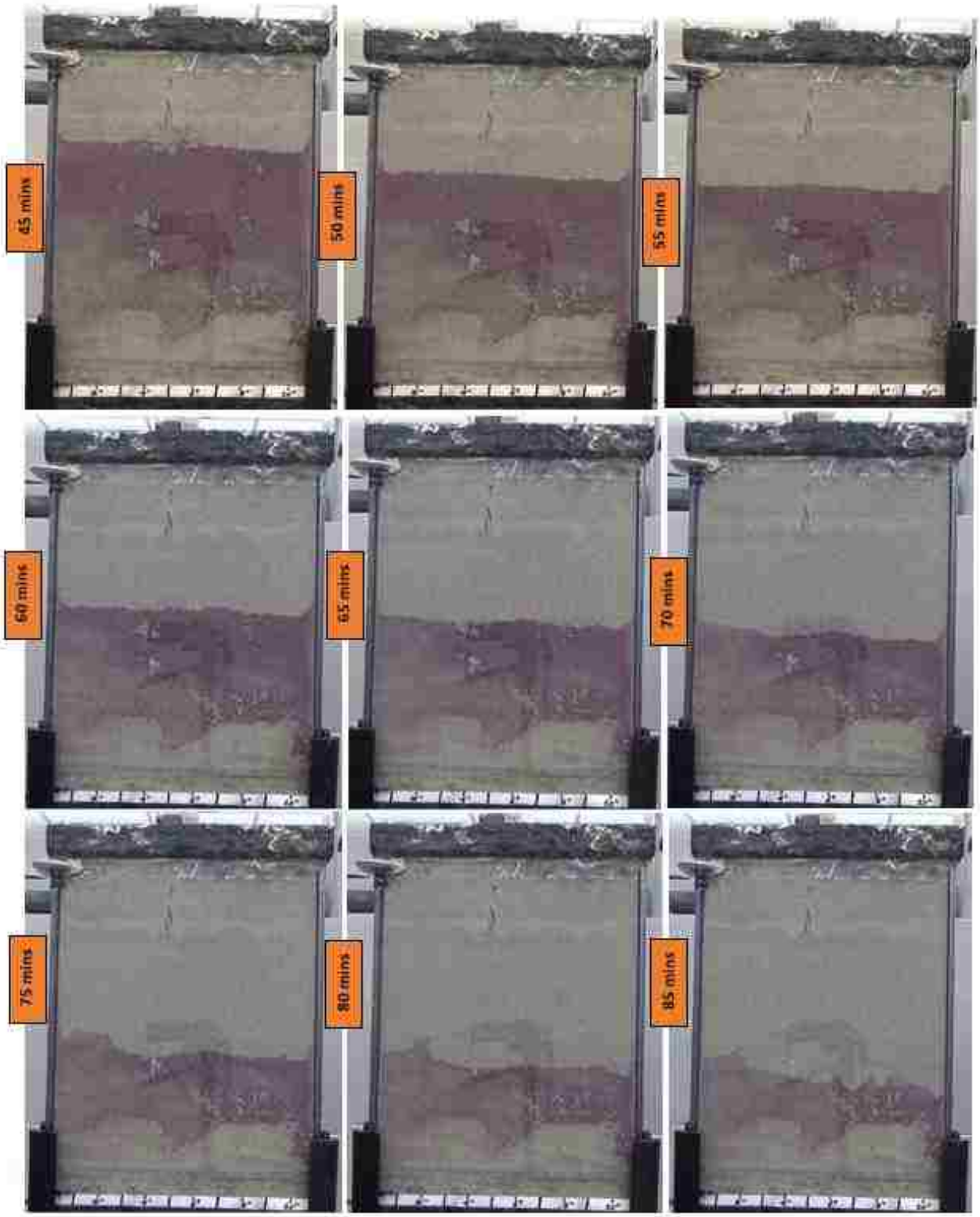

Figure 0.12. Front propagation for CO_2 flooding at 5 cc/min for Model # 1 (2 of 2)

The first set of images (Figure 5.9 and 5.10) of the propagation front is for N_2 flooding at 5cc/min at 5 min intervals for model# 1. The second set of images (Figure 5.11 and 5.12) of the propagation front is for CO_2 flooding at 5 cc/min at 5 min intervals for model # 1. The area in the model near the bottom of the model where no oil is visible is attributed to the fact that there is a small section of the model with higher grain size particles near the horizontal well. While the model is flooded with oil, the permeability near that region is expected to be higher hence causing that part of the model to be somewhat less oil saturated than the rest of the model. Similar to the observations from Mahmoud (2016), the oil drains from the model in an almost horizontal flood front as visible from the front propagation, further showing gravity as the dominating force for the flooding process with a density difference between the injected gas and oil.

This study compares the production of oil using different injection gases, namely nitrogen and carbon dioxide. In a previous study from (Ruiz, May 2006) the recovery rates for sandstone model were higher with injection of carbon dioxide gas. This is more prevalent in a reservoir as at higher temperature and pressure CO_2 has a higher solubility with oil and hence reduces the oil viscosity. Also, CO_2 tends to swell the oil which increases the relative oil permeability.

With this study, Nitrogen gas yields higher recovery for Gas Assisted Gravity Drainage application through all the experimental cases with carbonate rocks. In general, the production increase is in the range of ~2.5% - 5.5% total recovery. The recovery rates are summarized in Table 5.3. Especially for Model # 2, the oil recovery from nitrogen injection is quicker at lower pore volume gas injection than that of CO_2 injection for the same model (Figure 5.6 and 5.8). The difference in the results for the two models is discussed in the grain size effects section. The

results are somewhat in contrast to the expectations and can be described by the physical characteristics of Nitrogen vs. CO_2 gas. First, nitrogen has better injectivity in low permeability reservoirs. Carbonates tend to have lower permeability than sandstone reservoirs as discussed in the literature review section. Secondly, the lower molecular weight for nitrogen than that of carbon dioxide enables nitrogen to reach small pores in the system that can't be reached by carbon dioxide (Lwisa and Abdulkhalek, 2018). Carbon dioxide has a molecular weight of 44.01 whereas Nitrogen gas has a lower molecular weight of 28.01. The varying molar mass of the two gases leads to a varying density for the two gases. At standard temperature and pressure, Nitrogen gas has a density of 1.25 g/L while CO_2 has a density of 1.96 g/L. Similar observations were observed with nitrogen flooding for lab studies done by Koch and Hutchinson (1958) and related to the vaporization gas drive from nitrogen flooding. The mechanism drives the vaporization of the lighter oil components (C1 to C6) and hence can make nitrogen more effective for light oil with high methane concentration. However in this study, decane was used to represent oil.

Table 0.3. Comparison of incremental production from Nitrogen injection compared to Carbon dioxide injection

Model # 1 (Grain size = 300-425 µm)				
Nitrogen Gas Run #	**Total Recovery (%)**	**CO_2 Gas Run #**	**Total Recovery (%)**	**% Difference with N_2 injection vs. CO_2 injection**
Run N_2.5	73.34	Run C_2.5	70.87	2.47
Run N_5_1	80.05	Run C_5	75.09	4.96
Run N_5_2	78.63			
Run N_7.5	74.42	Run C_7.5	71.19	3.23
Model # 2 (Grain size = 600 µm)				
Run 2N_2.5	80.5	Run 2C_2.5	77.87	2.63
Run 2N_5_1	87.68	Run 2C_5	82.1	5.58
Run 2N_5_2	86.39			
Run 2N_7.5	87.07	Run 2C_7.5	83.3	3.77

5.3 Effect of Injection Rates

In this section of the study the effects of different injection rates are shown for both models. Gas injection rate is an important parameter as the amount of gas injected is dependent on the injection rate and the injection gas rate has a cost associated with it. Also, the gas injection rate has impact on the oil production rate, which in turn has cost implications for any project. From the three different injection rates used for the experiments, namely an injection rate of 2.5cc/min, 5 cc/min, and 7.5 cc/min, it was found that the optimal injection rate was at 5cc/min injection rate. The overall recovery was highest when using the 5 cc/min injection rate however, at a higher injection rate the recovery is faster which may also be important from an economic point of view. To showcase this, the results are also shown against the pore volume injection for Model # 1 for nitrogen and carbon dioxide gas injection in Figures 5.17 and 5.18. From the pore volume injection perspective, the slower injection rate has a lager recovery during gravity dominated flow or the earlier stages of recovery. This intuitively makes sense as slower injection rates allows the gas flood to penetrate more thoroughly as opposed to the faster injection rates. As Mahmoud (2006) described in his findings, the injection rate is also important as it determines whether the flow is gravity dominated or viscous dominated. In higher injection rates the pressure increases quickly which leads the viscous force to control the process. However, at higher pressure, CO_2 in particular will have a higher oil solubility which will further reduce the viscosity and lead to more film like drainage with higher displacement efficiency. The results found for carbonate materials show that the largest recovery is obtained at an intermediary injection rate. This could be due to the higher injection rates causing an earlier breakthrough and hence the overall recovery is slightly lower at the highest injection rate. The results for both

models with Nitrogen and Carbon dioxide injection are shown in the below charts, Figures 5.13 through 5.16.

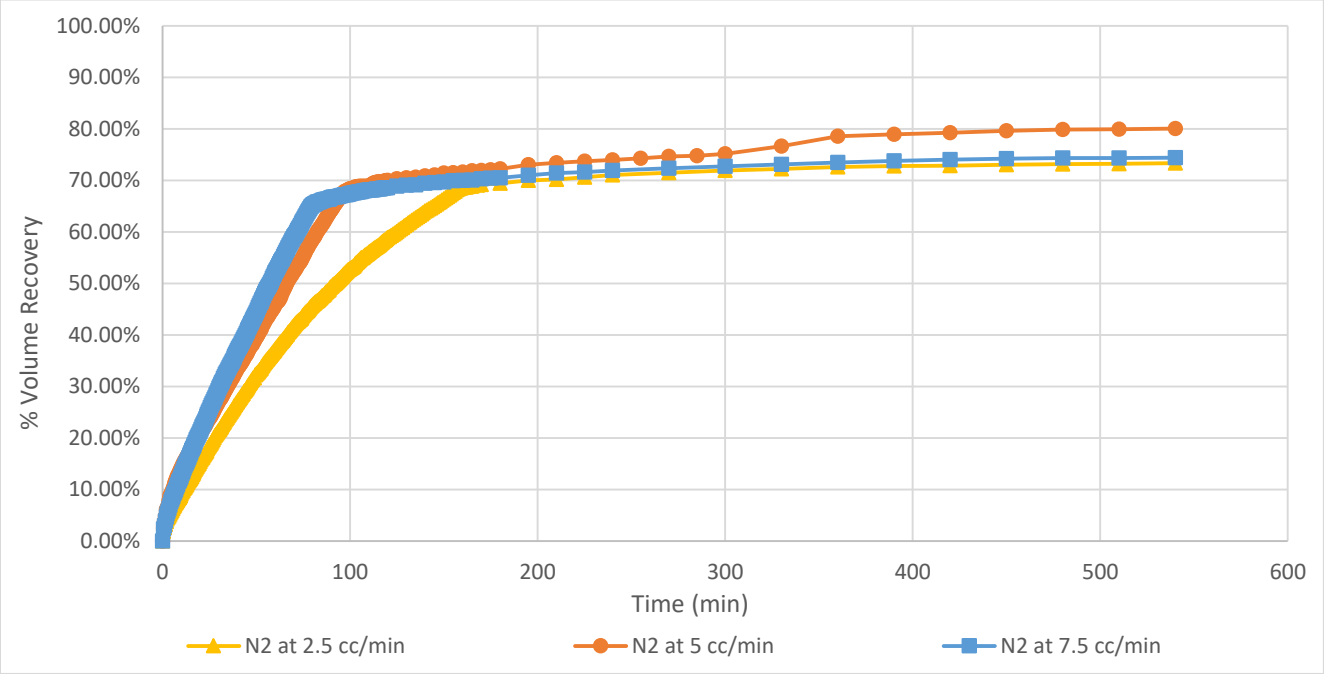

Figure 0.13. Oil recovery for Model # 1 (smaller grain size packing) with Nitrogen injection gas

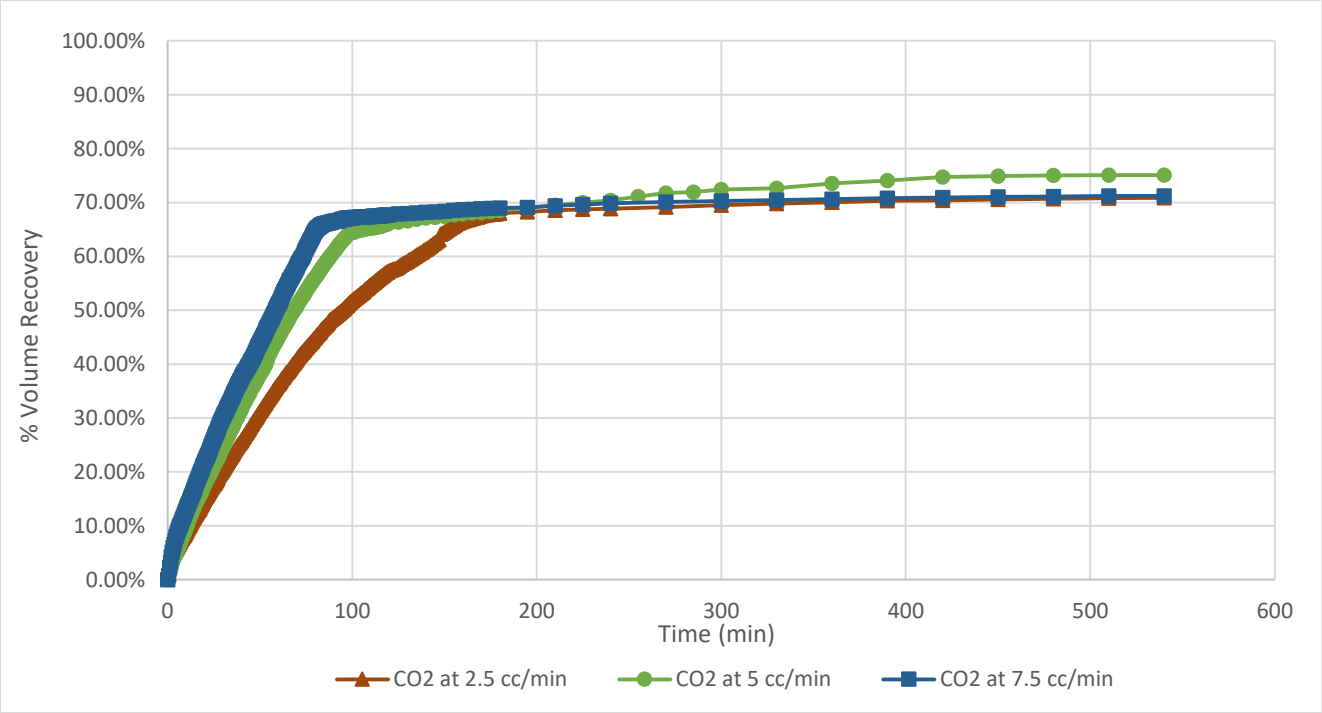

Figure 0.14. Oil recovery for Model # 1 (smaller grain size packing) with CO_2 injection gas

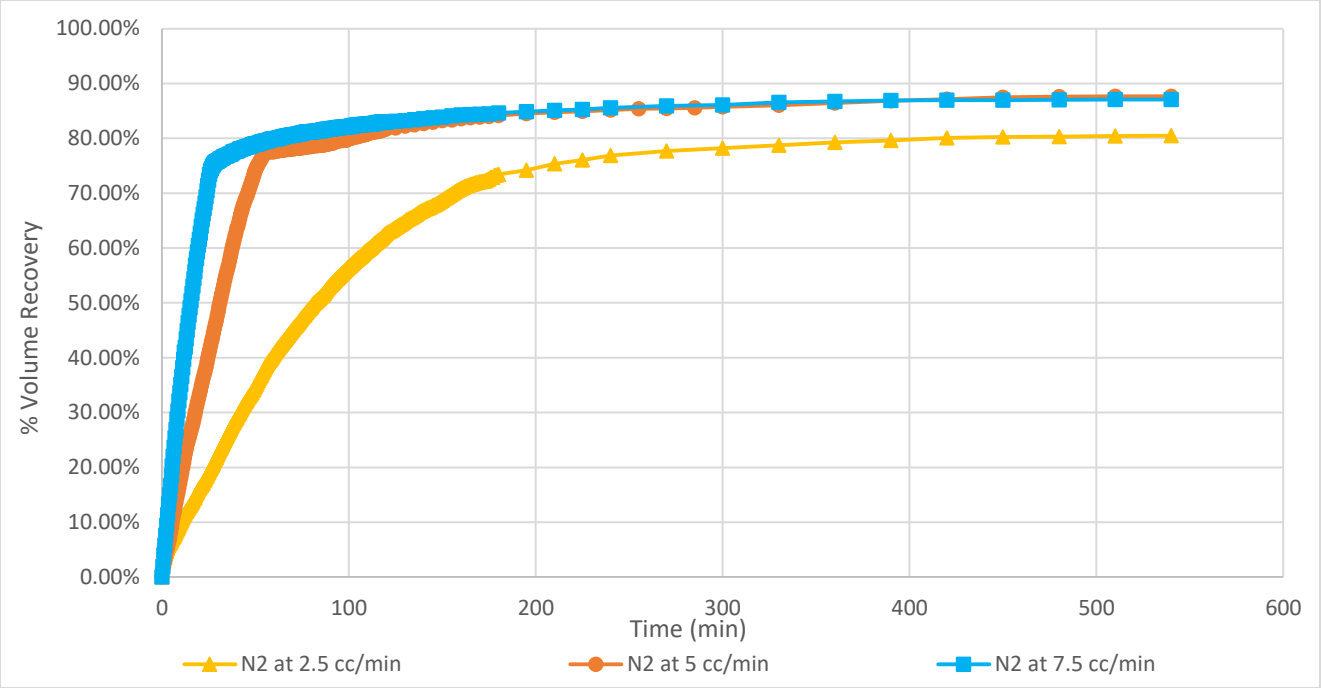

Figure 0.15. Oil recovery for Model # 2 (larger grain size packing) with Nitrogen injection gas

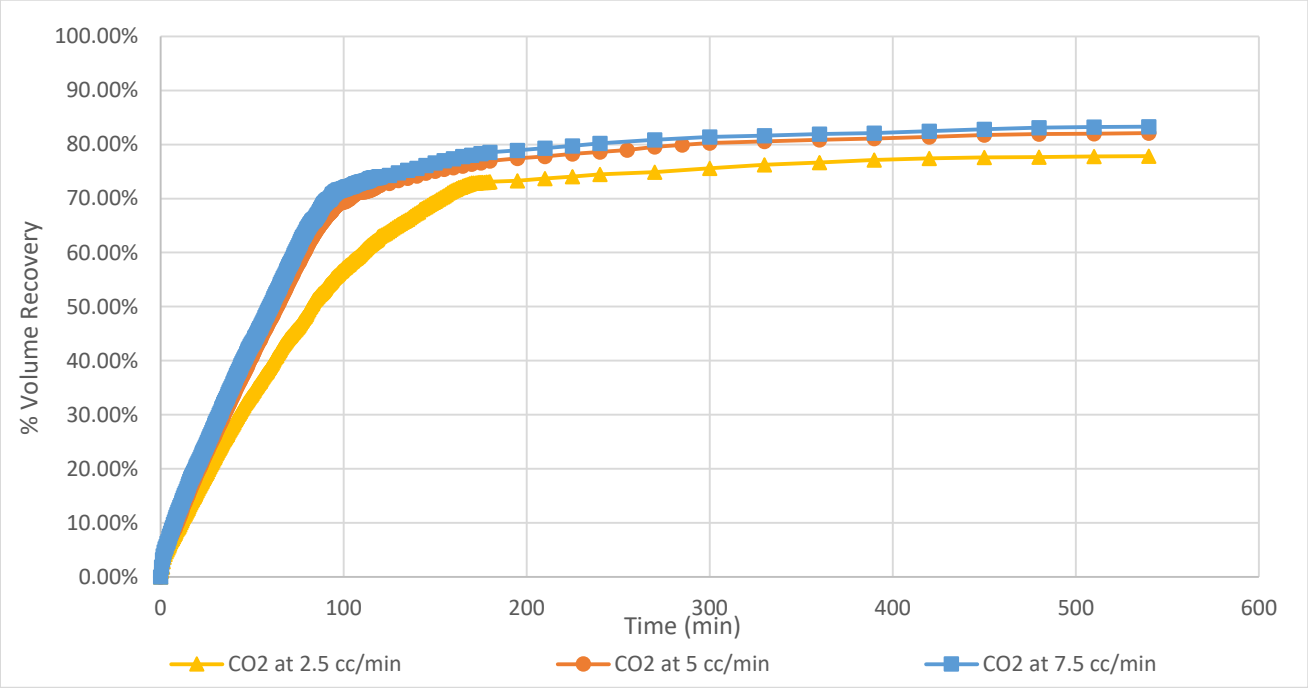

Figure 0.16. Oil recovery for Model # 2 (larger grain size packing) with CO_2 injection gas

Interestingly, model# 2 shows a very similar overall recovery at 5 cc/min and 7.5 cc/min. The higher porosity in the model leads to an earlier gas breakthrough which may cause the difference between Model # 1 and Model # 2. These effects are discussed further in the following section while comparing the grain size effect on the recovery rates. It is noted that the overall recovery rate is not significantly different to imply a clear relationship between the observed results.

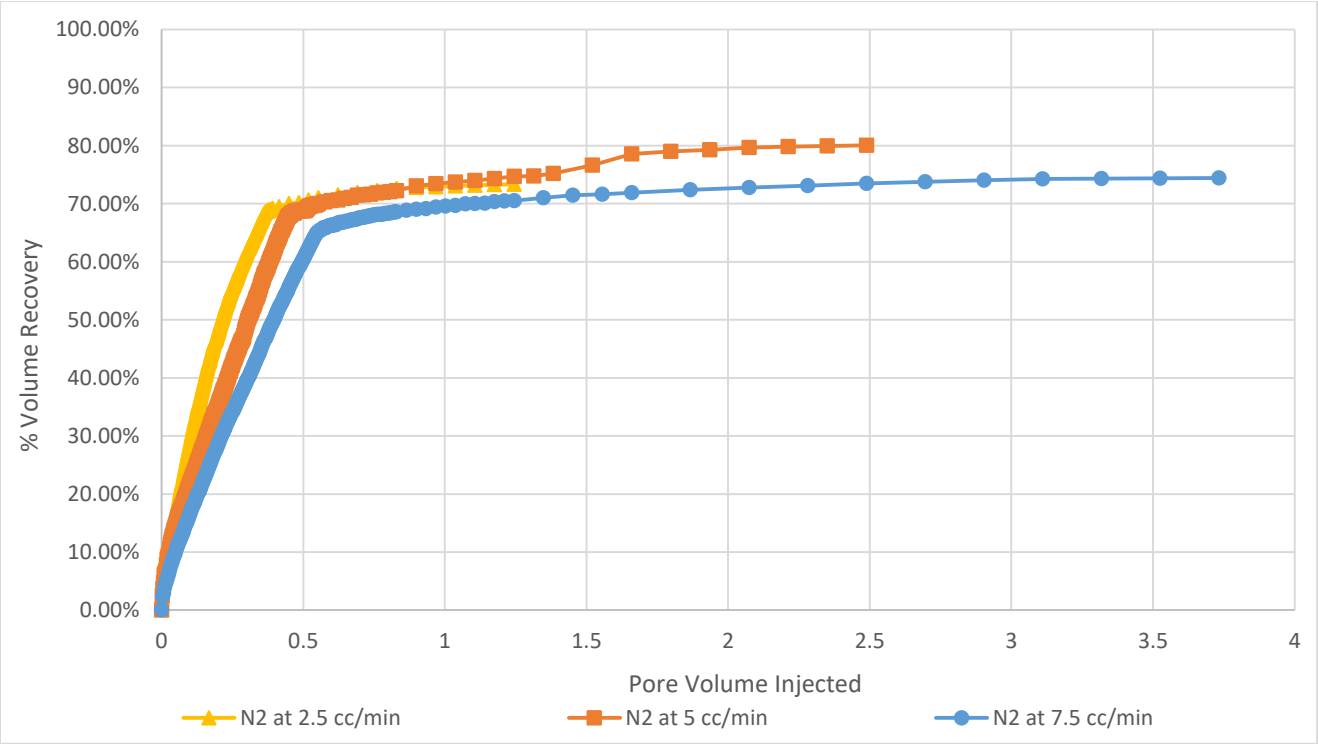

Figure 0.17. Oil recovery for Model # 1 (smaller grain size packing) with Nitrogen injection gas (PVI basis)

As seen from the above charts in Figure 5.17 and 5.18, from a pore volume injection basis the slower injection rates yields a better volumetric sweep and thus a higher initial recovery. The overall recovery is still highest at the intermediate injection rate and in order to keep the timings consistent for the experiments, the experimental runs were run for a similar time period, not similar gas injection volume. Section 5.5 discusses the impact of the pore volume injection with different gases used as injection gas.

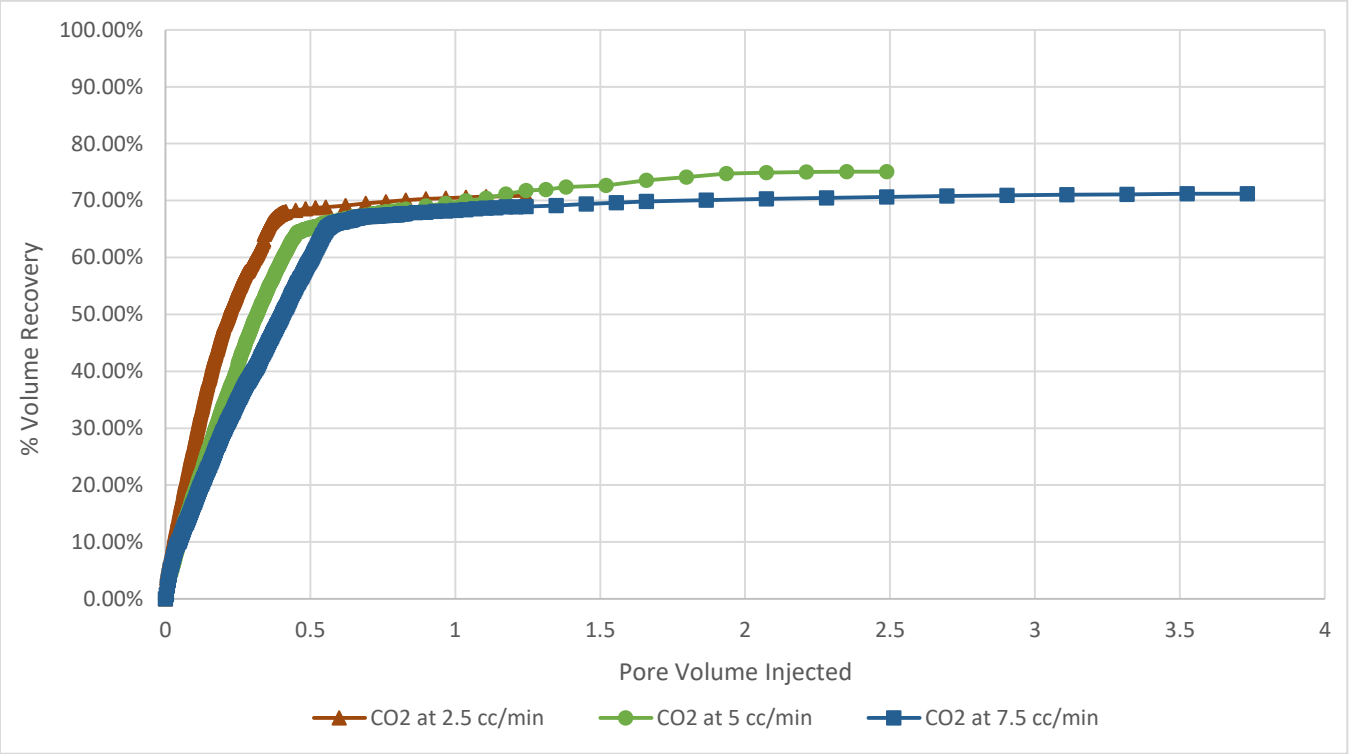

Figure 0.18. Oil recovery for Model # 1 (smaller grain size packing) with CO_2 injection gas (PVI basis)

5.4 Effect from Different Grain Size

The two models used for this study were packed with different grain size of carbonate material in order to observe the effects of varying the grain size on the overall recovery rates. The first model was packed with carbonate grain size of 300-425 μm with a 2" column of 600 μm particles near the horizontal well to allow for a gravel packing type effect and to ensure that none of the smaller diameter grains escape through the horizontal well. As a contrast, the second model was packed with 600 μm particles throughout the model. As hypothesized, the larger grain size yielded a higher porosity of 40.07%, while the first model with smaller grain size particles had a 34.2% porosity. This approximately 6% higher porosity in Model # 2 is further translated into higher recoveries for the same injection fluid and injection rate. A summary of the results is

shown in Table 5.4 below. The comparison shows a higher recovery across each run for the second model with an increased recovery of between 7% - 12.65%. The largest difference is at the 7.5 cc/min injection rate while the difference between 2.5 cc/min and 5cc/min is marginal.

Table 0.4. Comparison of incremental production between the two models

Nitrogen Injection				
Model # 1 (Grain size = 300-425 µm) Run #	**Total Recovery (%)**	**Model # 2 (Grain size = 600 µm) Run #**	**Total Recovery (%)**	**% Difference between Model # 1 and Model # 2**
Run N_2.5	73.34	Run 2N_2.5	80.5	7.16
Run N_5_1	80.05	Run 2N_5_1	87.68	7.63
Run N_5_2	78.63	Run 2N_5_2	86.39	7.76
Run N_7.5	74.42	Run 2N_7.5	87.07	12.65
Carbon Dioxide Injection				
Run C_2.5	70.87	Run 2C_2.5	77.87	7
Run C_5	75.09	Run 2C_5	82.1	7.01
Run C_7.5	71.19	Run 2C_7.5	83.3	12.11

The charts below in Figures 5.19 to 5.21 show the recovery profile for the pore volume gas injected for the two models comparing the overall recovery rate from the OOIP.

The recovery profiles clearly shows a faster and higher recovery for the model with larger grain size particles. This effect is related to the fundamental principles of the Carmen-Kozeny relationship for porous medium. The equation for calculating the absolute permeability is a function of the particle diameter and porosity and tortuosity.

$$k = \frac{D_p^2 \emptyset^3}{72\tau(1-\emptyset)^2}$$

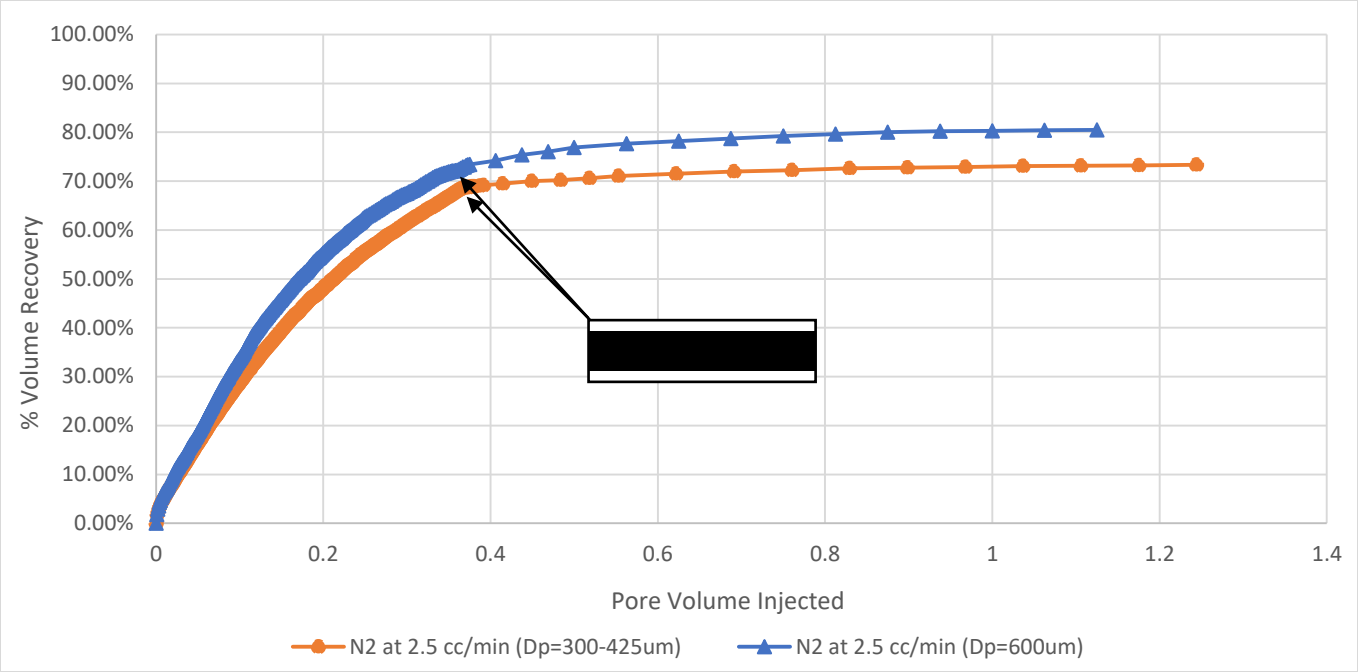

Figure 0.19. Oil recovery with Nitrogen injection for two different grain size

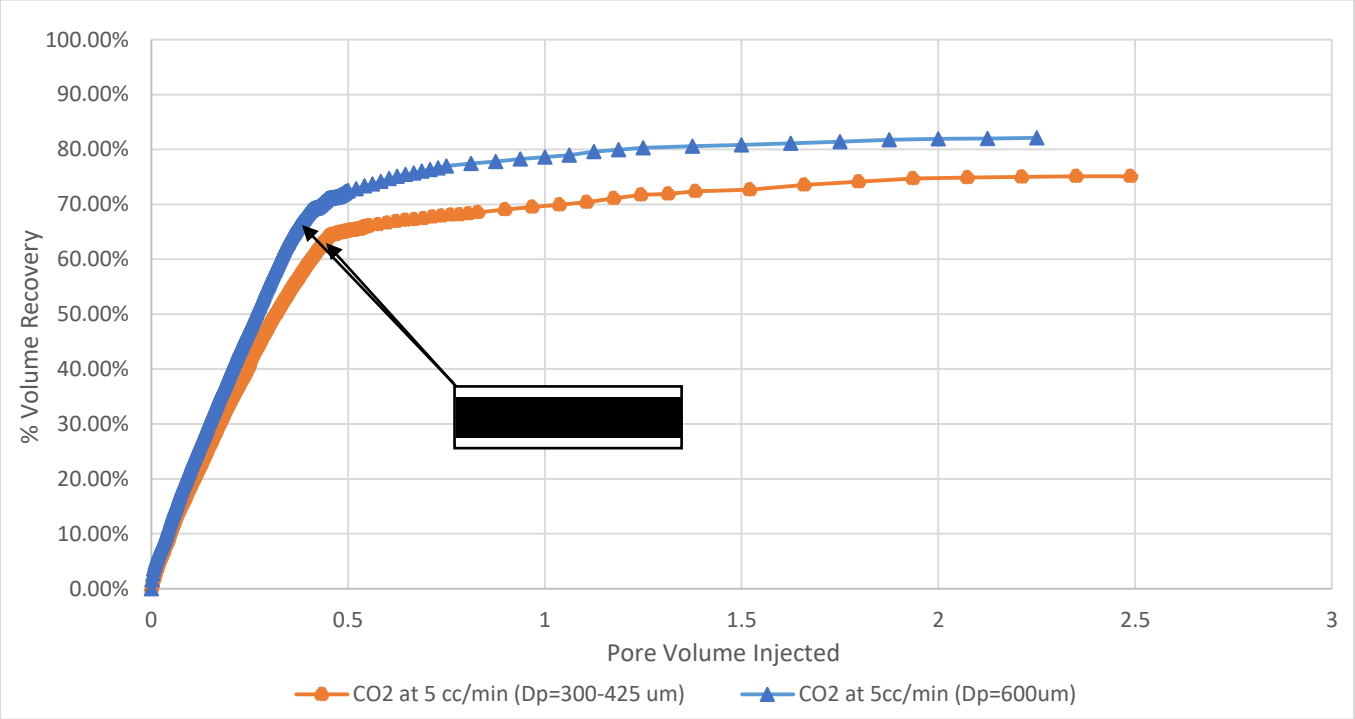

Figure 0.20. Oil recovery with Carbon dioxide injection for two different grain size

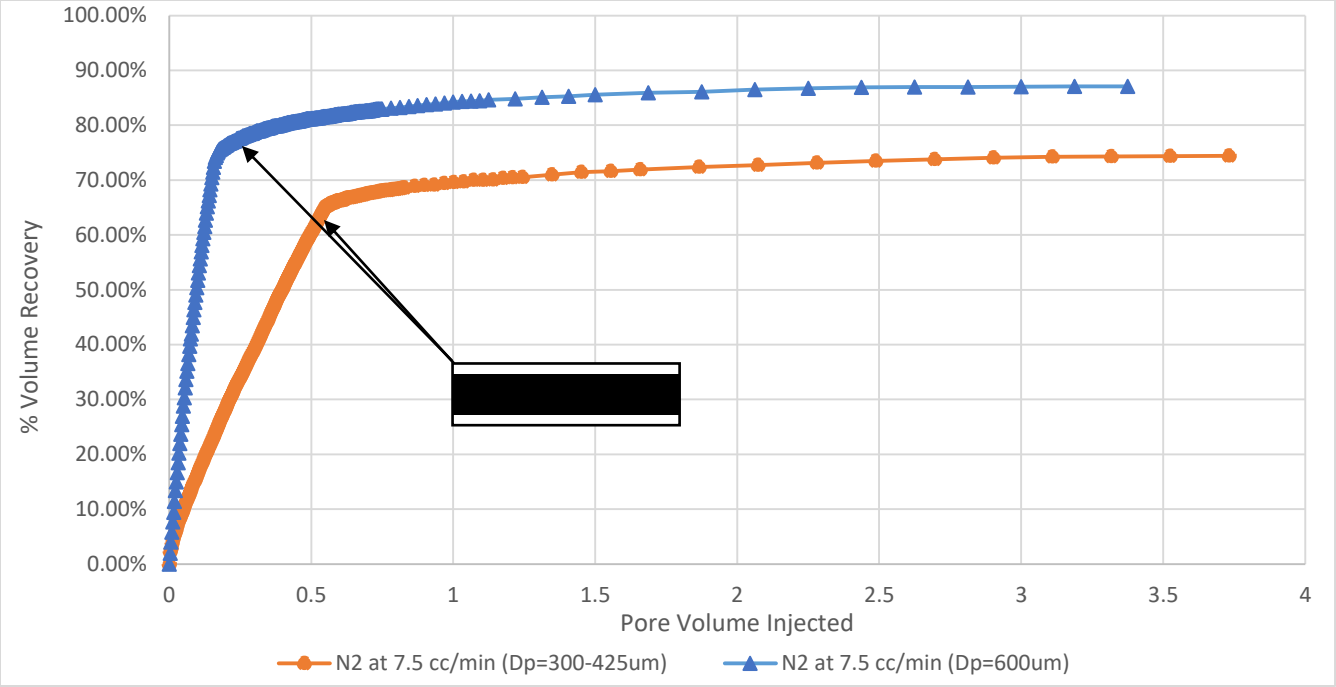

Figure 0.21. Oil recovery with Nitrogen injection for two different grain size

Permeability is a function of the square of particle size diameter and thus higher grain size tends to lead to a larger permeability which eventually leads to a larger oil recovery as seen above. In the study, Model # 2 has the larger grain size diameter with a higher porosity and higher permeability compared to Model # 1. These results vary from Ruiz's study (2006) where it was found that the larger grain size glass beads yielded lower recovery however, his results were unexpected in his study and were claimed to be because of "a departure from normal procedure for the packing of the physical model… The model was filled by introducing the glass beads into the cavity by hand-packing prior to assembly of the physical model along. This resulted in relatively tighter packing and, therefore, decreased porosity and permeability resulting in a decrease in oil recovery compared with the looser packed 0.13 mm porous media." (Ruiz, 2006). The results from this study confirmed higher recovery for larger grain size particles.

5.5 Effect of Type of Gas Injection & Gas Injection Rate on Oil Production

At the field scale, the gas injection rate is a very important consideration as that equals to both time and money spent for injecting any gas into the reservoir and get oil production in return. The summary of findings from the gas injection rate plotted as a function of the overall recovery percentage of OOIP has been shown in Figures 5.22 and 5.23 below. As per intuition, model 1 shows that the lower injection rate yields higher recovery of oil production in the early stages of injection (0-0.4 PVI) as the lower injection rate has a better front propagation that moves slower compared to the higher injection rates which may not fully sweep the model. This is valid for either carbon dioxide or nitrogen injection. This is also evident from the experimental runs from the visual analysis. There is slightly different observation for the second model from the results shown in Figure 5.23 where the nitrogen injection at higher injection rate (7.5 cc/min) yields higher production during the early injection stage (0-0.25 PVI).

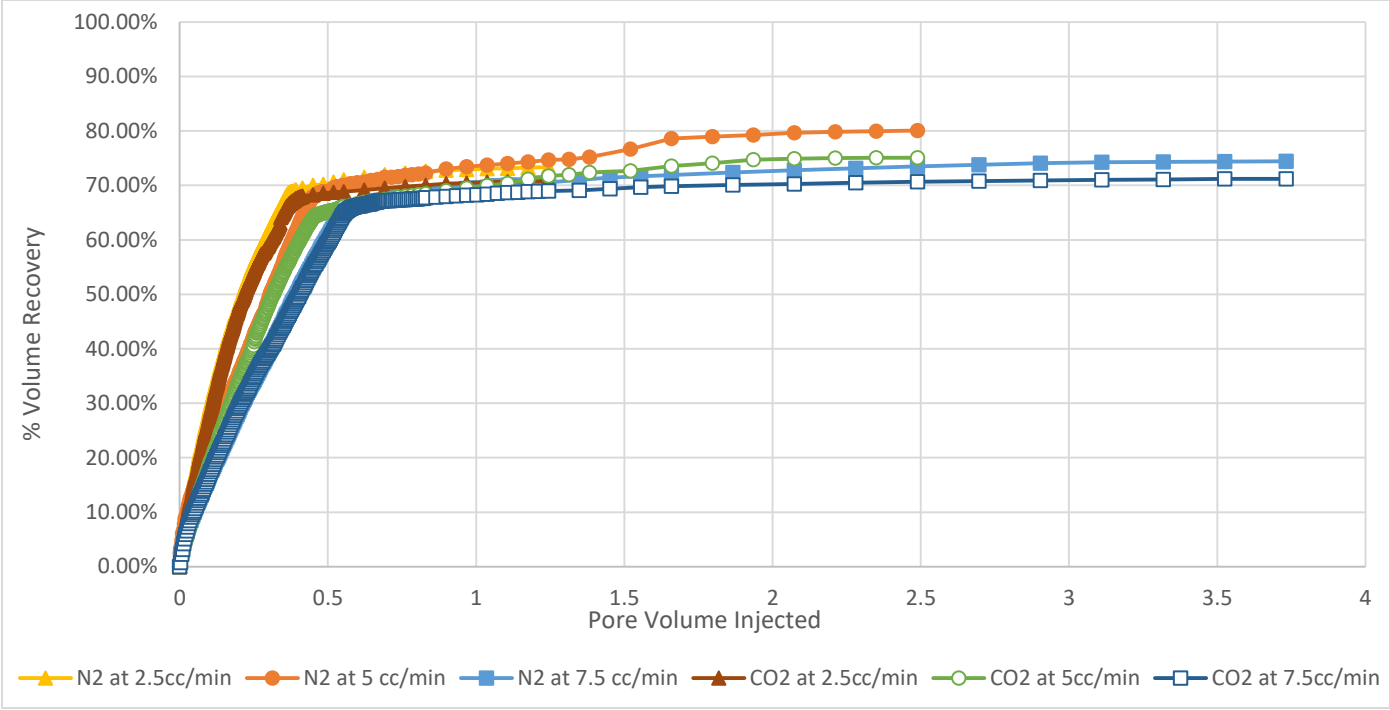

Figure 0.22. Effect of Gas type and injection rate on oil recovery for Model # 1 (D_p = 300-425 µm)

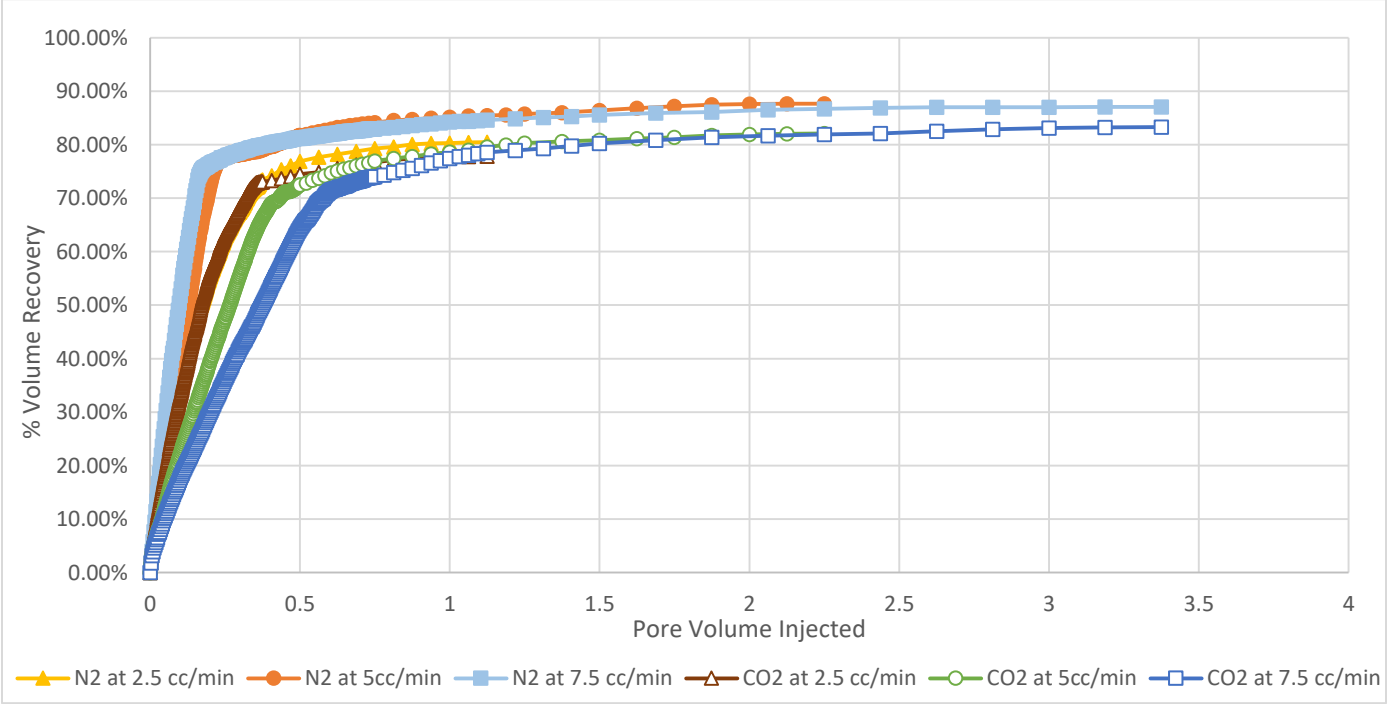

Figure 0.23. Effect of Gas type and injection rate on oil recovery for Model # 2 (D_p = 600 µm)

In addition to the gas injection volume vs. recovery, the below charts in Figure 5.22 and 5.23 show the percentage of volume recovery vs. time on a log scale. This analysis shows the recovery from a more enhanced time scale for early production and most importantly shows the gravity dominated flow in the beginning of the production. These results show similarities to observations from Mahmoud's study (2006) as three different mechanisms of oil recoveries: Darcy-type displacement until gas breakthrough, gravity drainage after breakthrough, and film drainage in the gas invaded zones. There is a remarkable difference between model 1 and model 2 results though and as discussed in the grain size effects section the larger grain size model has a general tendency of higher production throughout the study.

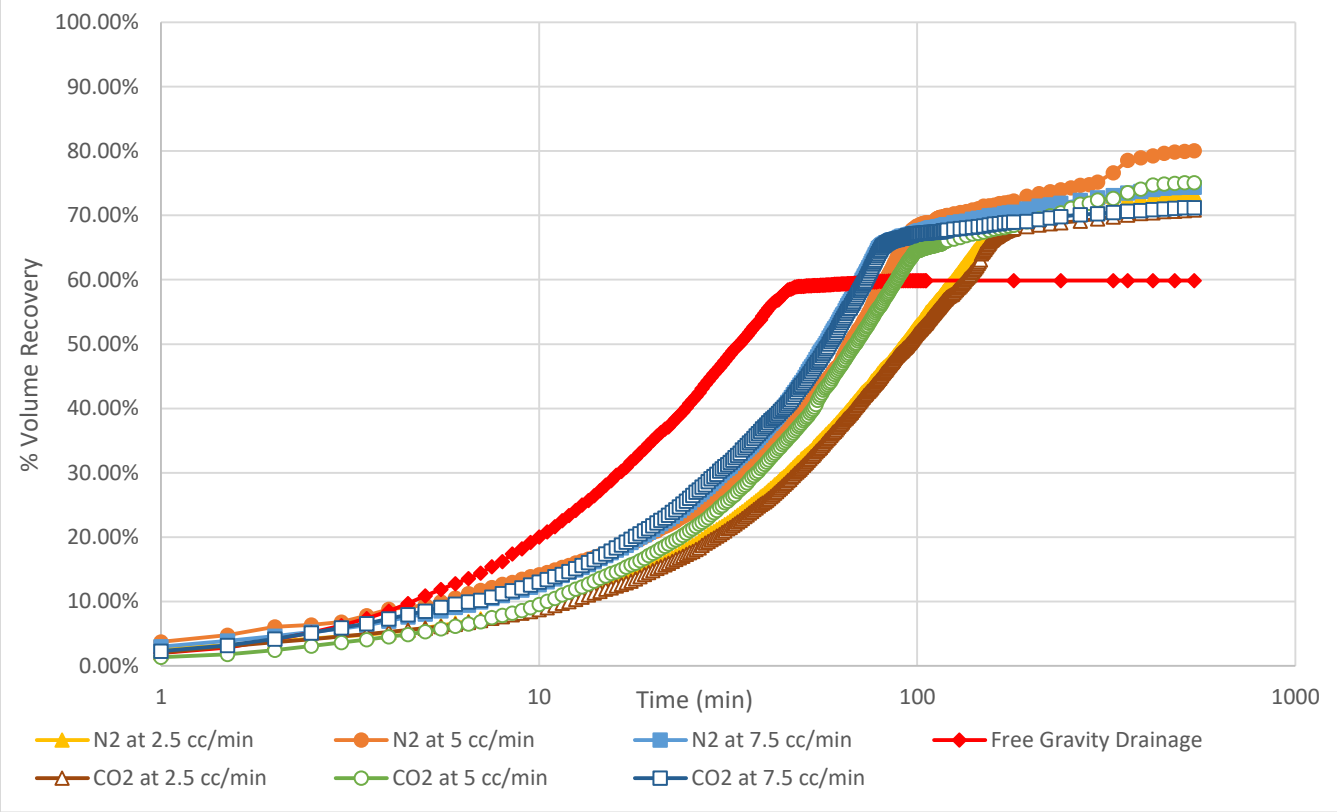

Figure 0.24. Oil Recovery vs. Time on a log scale for Model # 1 (D_p = 300-425 μm)

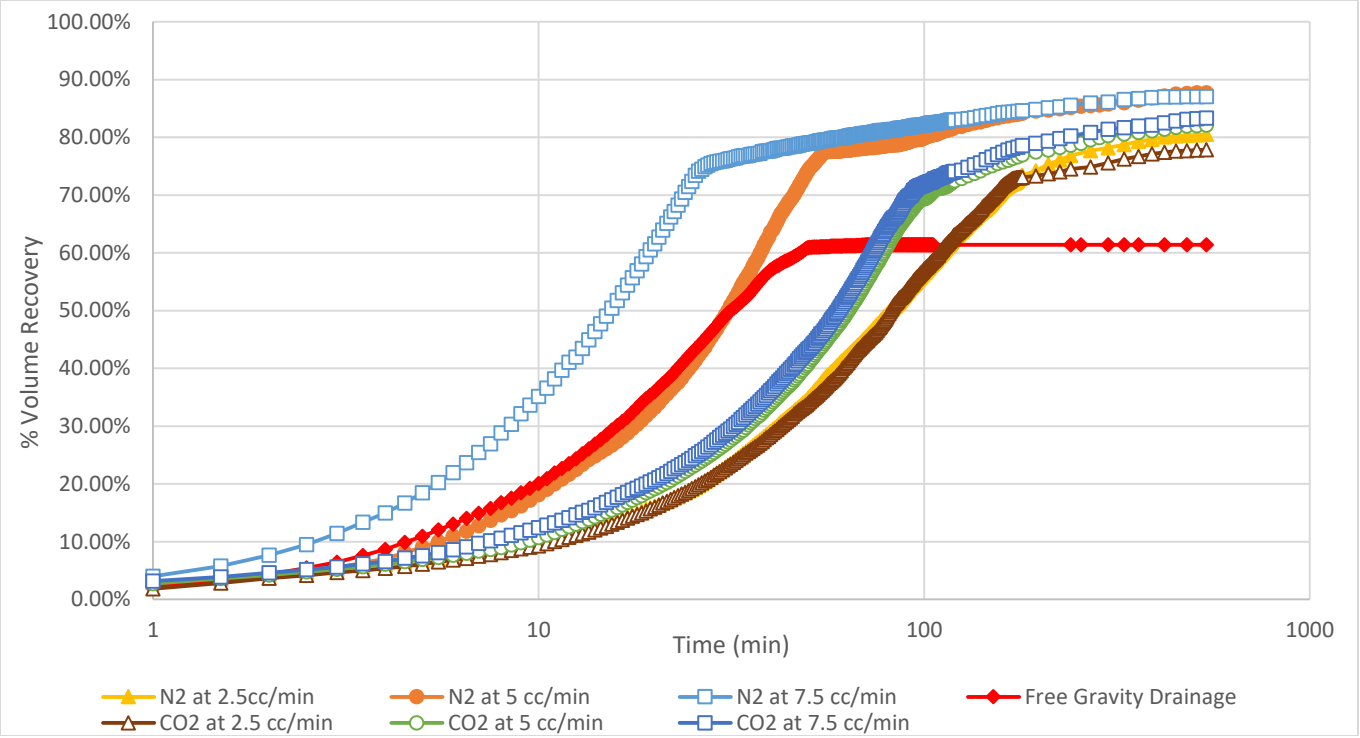

Figure 0.25. Oil Recovery vs. Time on a log scale for Model # 2 (D_p = 600 μm)

Additionally, using the dimensional analysis, a time scale analysis has been done to compare the results from the lab scaled models to a prototype field using the dimensionless time expression below. The expression for dimensionless time (t_D) for gravity drainage process as discussed in the literature review section, is shown again for reference.

$$t_D = \frac{KK_{ro}^{o}\Delta\rho g/g_c}{h\emptyset\mu(1-S_{or}-S_{wi})}\,t$$

The dimensionless time expression t_D (Miguel et al, 2004), the variables used are as follows:

K is the absolute permeability,

K_{ro}^{o} is the end-point relative oil permeability,

$\Delta\rho$ is the fluid density difference,

g is the Newtonian gravity acceleration,

g_c is the gravity acceleration conversion factor,

h is the height of the porous media,

ϕ is the porosity,

μ is the viscosity of oil (decane in the experimental case),

S_{or} is the residual oil saturation,

S_{wi} is the initial water saturation, and

t is time

Using the dimensionless time and comparing the results found from Sharma (2005), helps visualize the results for the GAGD experiments in carbonate to field values and also compares it to previous lab scale studies using sandstone as the porous medium. Similar to the gravity drainage field used by Sharma, the Dexter Hawkins field data is used to compare the time from the lab models to the field data. The properties from the Dexter Hawkins field used for dimensionless time calculations are summarized in Table 5.5 and are taken from Carlson (1988) as used by Sharma (2005).

Table 0.5. Field Scale Properties used for the dimensionless time calculations

Field Scale Properties	**Value**
Absolute Permeability K (D)	1.2
End-point relative oil permeability (K_{ro}^{o})	0.31
Oil Density (ρ_o(kg/m^3))	908
Gas Density (ρ_g (kg/m^3))	10
ϕ	0.25
μ_o	3.75
S_{wi}	0.27
S_{or}	0.1
h (ft)	175

The field data from the Dexter Hawkins field used for the scaling calculations are for a field that was subject to gravity drainage for 15 years with an 81% oil recovery under gravity-stable gas injection. Table 5.6 is a comparison of the values obtained from the lab scale model at the 10 minute experimental value to a corresponding time to the field. The values obtained from the dimensional time analysis indicate a performance of the first 10 minutes of the lab scaled experiments to be roughly 3-4 months in the field. As seen from the Figures 5.25 and 5.26 with oil production on a log scale, the lab scale models reach their breakthrough point within the first 100 minute of the experiments. These values are also similar to the values obtained by Sharma from his study as shown in Figure 5.26. Thus, it can be observed that the physical model experiments compares with the field study and previous experimental study.

Table 0.6. Scaled time for the Dexter Hawkins field using dimensional analysis at 10 minutes of lab scale model

Nitrogen Injection			
Model # 1 (Grain size = 300-425 μm) Run #	Days in Dexter Hawkins Field for 10 minutes	Model # 2 (Grain size = 600 μm) Run #	Days in Dexter Hawkins Field for 10 minutes
Run N_2.5	91 days	Run 2N_2.5	117 days
Run N_5	83 days	Run 2N_5	107 days
Run N_7.5	90 days	Run 2N_7.5	106 days
Carbon Dioxide Injection			
Run C_2.5	95 days	Run 2C_2.5	121 days
Run C_5	89 days	Run 2C_5	114 days
Run C_7.5	95 days	Run 2C_7.5	112 days

Run Name	Gas injection mode	Gas Injection rate	Grain size	Time in physical model (minutes)	Equivalent time in Dexter Hawkins Field in Days
CP1	Primary	4 psi	0.5mm	10	106 days
CP2	Primary	4 psi	0.15mm	10	113 days
CR1	Primary	20 cc/min	0.15mm	10	127 days
CR2	Primary	20 cc/min	0.065mm	10	119 days
CR3	Primary	20 cc/min	0.15mm	10	110 days
CR4	Primary	20cc/min	0.15mm	10	69 days
CR5	Primary	50 cc/min	0.15mm	10	113 days
CR6	Primary	5 cc/min	0.15mm	10	120 days
CR7	Primary	400 cc/min	0.15mm	10	106 days
CR8	Primary	200 cc/min	0.15mm	10	95 days
CR9	Primary	300 cc/min	0.15mm	10	99 days
TF1	Secondary	20 cc/min	0.15mm	10	183 days
TF2	Secondary	50 cc/min	0.15mm	10	204 days
TF3	Secondary	5 cc/min	0.15mm	10	161 days
TF4	Secondary	400 cc/min	0.15mm	10	153 days

Figure 0.26. Scale-Up of Time using Dimensional Analysis from a study done by Sharma 2005

6. CONCLUSIONS AND FUTURE RECOMMENDATIONS

6.1 Conclusions

The purpose of this study was to conduct physical model experiments for the GAGD process with carbonate porous media and to study the effects of injection rate, injection gas type, and grain size variations on the overall oil recovery. A 2-D Hele-Shaw type model was used to conduct the experiments for the study using carbonate rocks for the porous medium and decane and water were used to mimic natural reservoir conditions. The GAGD process was performed in a secondary displacement mode (tertiary mode was impractical for the model used) using carbon dioxide or nitrogen gas as injection gas. Different gas injection rates were used for the experiments. From the above results section, a summary of the findings and conclusions from this study are listed below:

- The GAGD process is valid and successful in crushed carbonate rocks as used in this study for the porous medium within the physical models.
- Gravity force is dominantly present in the recovery process and from the visual findings shown, forms a very stable front that propagates through the model and minimizes viscous fingering.
- From the carbonate model studies for the GAGD process, it was found that nitrogen produced higher recovery in all instances with a range of 2.5% - 5.5% incremental recovery compared to carbon dioxide injection.
- The injection rate was varied for the study using three different injection rates to mimic slow, intermediate, and faster injection rates. It was found that the ultimate oil recovery for all cases except one, were higher at the intermediate injection rate. The intermediate injection rate provides a balance between the front propagation and the higher pressures

at the higher injection rate which may lead to an earlier breakthrough. It must be noted that the Model # 1 was packed with a higher grain size particles near the bottom of the well and thus may cause some entrance and exit effects.

- The most significant impact was found to be due to the particle size of carbonate material for this study. The model with the larger grain size diameter had a higher porosity and permeability and also yielded the highest recovery rate with an increased recovery rate between 7% to 12.6% from the various injection rates and injection gas. The overall recovery range was 70.9% to 87.7% of OOIP.

6.2 Future Recommendations

The importance of the application of GAGD process in carbonate reservoirs is vital. This study proves that the process is relevant and useful for higher recovery in carbonate reservoirs and can work successfully as a secondary or tertiary oil recovery method. As a result of the model design, this study did not conduct experiments in tertiary mode and this is certainly something that can be performed for a future study. The author would also like to note that the carbonate material was crushed and sieved in order to pack the material in the model used for this study. This results in the loss of some fundamental properties of the material however, the results are still valid as the carbonate material retains the chemical characteristics. Also, design parameters for this study can be further proven with other similar studies and simulation efforts. The vast difference that was found in the grain size diameter, for example, can be further narrowed down with using more models with more grain size variations. Further, even though the study shows Nitrogen as a more effective injection gas, it is the author's belief that carbon dioxide is still a better option due to the added benefit of environmental impact from carbon dioxide injection for oil recovery. There are also economic incentives for carbon injection that

would mitigate the marginal incremental recovery from nitrogen injection. A future study can consider the cost-benefit of carbon dioxide injection in conjunction with the latest incentive policy for applicable region of the world.

REFERENCES

Adibhatla, B. and Mohanty, K.K.: "Oil Recovery From Fractured Carbonated by Surfactant-Aided Gravity Drainage: Laboratory Experiments and Mechanistic Simulations", Paper SPE 99773 Presented at the 2006 SPE/DOE Symposium on Improved Oil Recovery, Tulsa, April 22-26.

Barwis, J.W., McPherson, J.G., and Studlick, J.R. *Sandstone Petroleum Reservoirs*. New York: Springer-Verlag New York, 1990. p. 583

Carbonate Reservoirs: Meeting unique challenges to maximize recovery, Schlumberger Brochure p.2. Can be accessed from http://www.slb.com/resources/other_resources/brochures/technical_challenges/carbonates/br_unique_challenge.aspx

Caudle, B.H and Dyes, A.B. (1958). "Improving Miscible Displacement by gas-Water Injection" Petroleum Transactions, AIME, Vol. 213, p. 281-283.

Choquette, P. W. and Pray, L. C. (1970). Geological nomenclature and classification of porosity in sedimentary carbonates: AAPG Bulletin, v. 54, p. 207– 250.

Ehrenberg, S. N. and Nadeau, P. H. (April 2005). Sandstone vs. carbonate petroleum reservoirs: A global perspective on porosity-depth and porosity-permeability relationships: AAPG Bulletin, v. 89, No. 4, p. 435-445.

Geertsma, J., Croes, G.A., and Schwarz, N. (1956) "Theory of Dimensionally Scaled Models of Petroleum Reservoirs", Petroleum Transactions, AIME, Vol. 207, p. 118-127.

Jarrell, P.M., Fox, C.E., Stein, M.H., Webb, S.L., Johns, R.T., Day, L.A. "Practical Aspects of CO_2 Flooding", SPE Monograph Series; Society of Petroleum Engineers: Richardson, TX, USA, 2002; Volume 22, pp. 220–231.

Kelly, William Dr. Summary transcription from Dr. Kelly (Associate Director, New York State Geological Survey). Accessed from the web at www.devonianstone.com/SandstoneLimestone.pdf

Kock, H. A. and Hutchinson, C. A. (1958) "Miscible Displacements of Reservoir using flue gas", J. Pet. Tech. 7-19; Trans. AIME p. 213.

Kulkarni M. M. (July 2005). Multiphase Mechanisms and Fluid Dynamics in Gas Injection Enhanced Oil Recovery Processes (Doctoral dissertation) Retrieved from the Louisiana State University Electronic Thesis & Dissertation Collection. (ETD 07152005-101224)

Kuuskraa, V.A., Koperna, G.J.: "Evaluating the Potential for 'Game Changer' Improvements in Oil Recovery Efficiency Using CO_2 EOR", U.S. Department of Energy: Washington, DC, USA, 2006.

Lewis, O.J. (1942). "Gravity drainage in Oil Fields," Trans. A.I.M.E., volume 155, p. 133.

Lovoll, G., Meheust, Y., Maloy, K. J., Aker, E., and Schmittbuhl, J. (2005) "Competition of gravity, capillary and viscous forces during drainage in a two-dimensional porous medium, a pore scale study", Elsevier Energy, Vol. 30, p. 861-872.

Lwisa, E. G. and Abdulkhalek, A. R. (2018) "Enhanced oil recovery by nitrogen and carbon dioxide injection followed by low salinity water flooding for tight carbonate reservoir: experimental approach", IOP Conf. Ser.: Mater. Sci. Eng. 323 012009.

Mahmoud, T. N. (July 2006). Demonstration and Performance Characterization of the Gas Assisted Gravity Drainage (GAGD) Process Using a Visual Method (Master's Thesis). Retrieved from the Louisiana State University Electronic Thesis & Dissertation Collection. (ETD 07102006-102745)

Manrique, E.J., Muci, V.E., and Gurfinkel, M.E.: "EOR Field Experiences in Carbonate Reservoirs in the United States", Paper SPE 100063 Presented at the 2006 SPE/DOE Symposium on Improved Oil Recovery, Tulsa, April 22-26.

Maroufi, P., Ayatollahi, S., Rahmanifard, H., Jahanmiri, A., and Riazi, M. (March 2013). "Experimental Investigation of Secondary and Tertiary Oil Recovery from Fractured Porous Media" Journal of Petroleum Exploration and Production Technology, Vol. 3, p. 179-188.

Miguel-Hernandez, N., Miller, M.A and Sepehrnoori, K. (November 2004). "Scaling Parameters for Characterizing Gravity Drainage in Naturally Fractured Reservoirs", Presented at the 2004 SPE International Conference, Puebla, Mexico, 8-9 November, 2004.

Moore, C. H. *Carbonate reservoirs porosity evolution and diagenesis in a sequence stratigraphic framework.* Amsterdam, Elsevier, 2001. 444 p.

Morse, J. W. and Mackenzie, F. T. *Geochemistry of Sedimentary Carbonates*. Elsevier Science Publishers: New York, NY, USA, 1990. p. 373-446.

Muskat, M. Physical Principles of Oil Production. New York City: McGraw-Hill Book Co. Inc. 1949.

PennEnergy, "Enhanced Oil Recovery (EOR) Survey 2014", Summary, April 1, 2014.

Rao, D. N. Gas-Assisted Gravity Drainage Process for Improved Oil Recovery. United States patent 8,215,392 B2, July 2012.

Rao, D.N. (Feb 2001). "Gas Injection EOR- A new meaning in the new millennium" Invited article for the distinguished author series, Journal of Canadian Petroleum Technology, Vol. 40, No.2, p. 11-18.

Rao, D.N., Ayirala, S.C., Kulkarni, M.M., Paidin, W.R., Mahmoud, T.N.N., Sequeira, D.S., Sharma, A.P., "Development of Gas-Assisted Gravity Drainage Process for Improved Light Oil Recovery", Final Technical Report 15323R15 (October 1, 2002 – September 30, 2006) submitted to US-Department of Energy, Cooperative Agreement No. DE-FC26-02NT15323, December 2006.

Rao, D.N., Xu, Q., Ayirala, S.C., Kulkarni, M.M., Sharma, A.P. "Development and Optimization of Gas-Assisted Gravity Drainage (GAGD) Process for Improved Light Oil Recovery", Annual Technical Progress Report, October 2003.

Ruiz, P. W. (May 2006). Physical Model Study of the effects of wettability and fractures on Gas Assisted Gravity Drainage (GAGD) Performance (Master's Thesis).

Saffman P. G. and Taylor G. "The penetration of a fluid into a porous medium or Hele-Shaw cell containing a more viscous liquid", Proceedings of the Royal Society of London, Series A, 1958; Vol. 245 p. 312–329.

Saikia, B. D. and Rao, D. N. Gas-Assisted Gravity Drainage – A New Process for CO_2 Sequestration and Enhanced Oil Recovery. Louisiana State University. Accessed from www.pete.lsu.edu

Scholle, P.A. & Halley, R.B. (1985). "Burial diagenesis: out of sight, out of mind (porosity-depth relationships)!" Carbonate cements. Society Economic Paleontologists and Mineralogists Special Publication 36, p. 309-334.

Sharma, A. P. (August 2005). Physical Model Experiments of the Gas-Assisted Gravity Drainage Process (Master's Thesis). Retrieved from the Louisiana State University Electronic Thesis & Dissertation Collection. (ETD 06152005-140544)

Smith, T. (2014). "Test Sieving Methods: Guidelines for Establishing Sieve Analysis Procedures", West Conshohocken, PA: ASTM International.

Stalkup, F.I., "Miscible displacement", SPE Monograph Series; Society of Petroleum Engineers: Dallas, TX, USA, 1984, p. 204.

Terwilliger, P.L., Wilsey, L.E., Hall, H.N. Bridges, P.M., and Morse, R. A. "An experimental and theoretical investigation of gravity drainage performance**",** Petroleum Transactions, AIME, 1951. Vol. 192, p. 285-296.

APPENDIX A: PRESSURE DATA FROM THE EXPERIMENTS

As noted in the experimental procedure section, the pressure data is collected sparsely throughout the experiments, generally at the 5 minute intervals for the experiments conducted. The pressure was minimal in all cases while injecting gas, never exceeding over 1 psi. Below image shows the pressure data from the Model # 1 with smaller grain size diameter with Nitrogen injection at 5 cc/min. The breakthrough was noted to be at 107 minutes for this case.

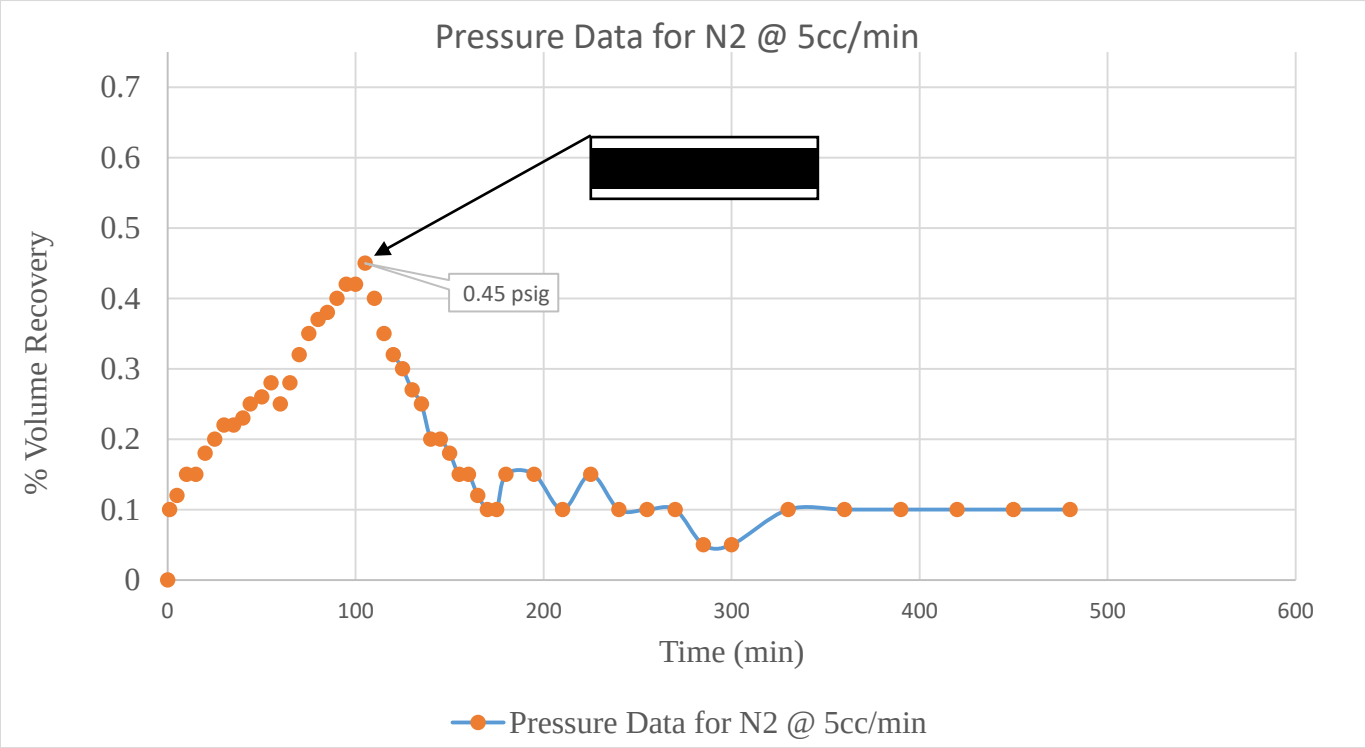

APPENDIX B: XRD ANALYSIS OF THE INDIANA LIMESTONE

XRD Analysis-powder reflection analysis-performed on the limestone sample used for packing the model, shows a composition of 98% Calcium carbonate material and 2% Silicon dioxide. The analysis was performed at the LSU Shared Instrumentation Facility (SIF) labs with the assistance of the staff at the SIF. The PANalytical Empyrean X-Ray Diffractometer at the SIF was used for the analysis. Below image are the results produced from the powder reflection analysis.

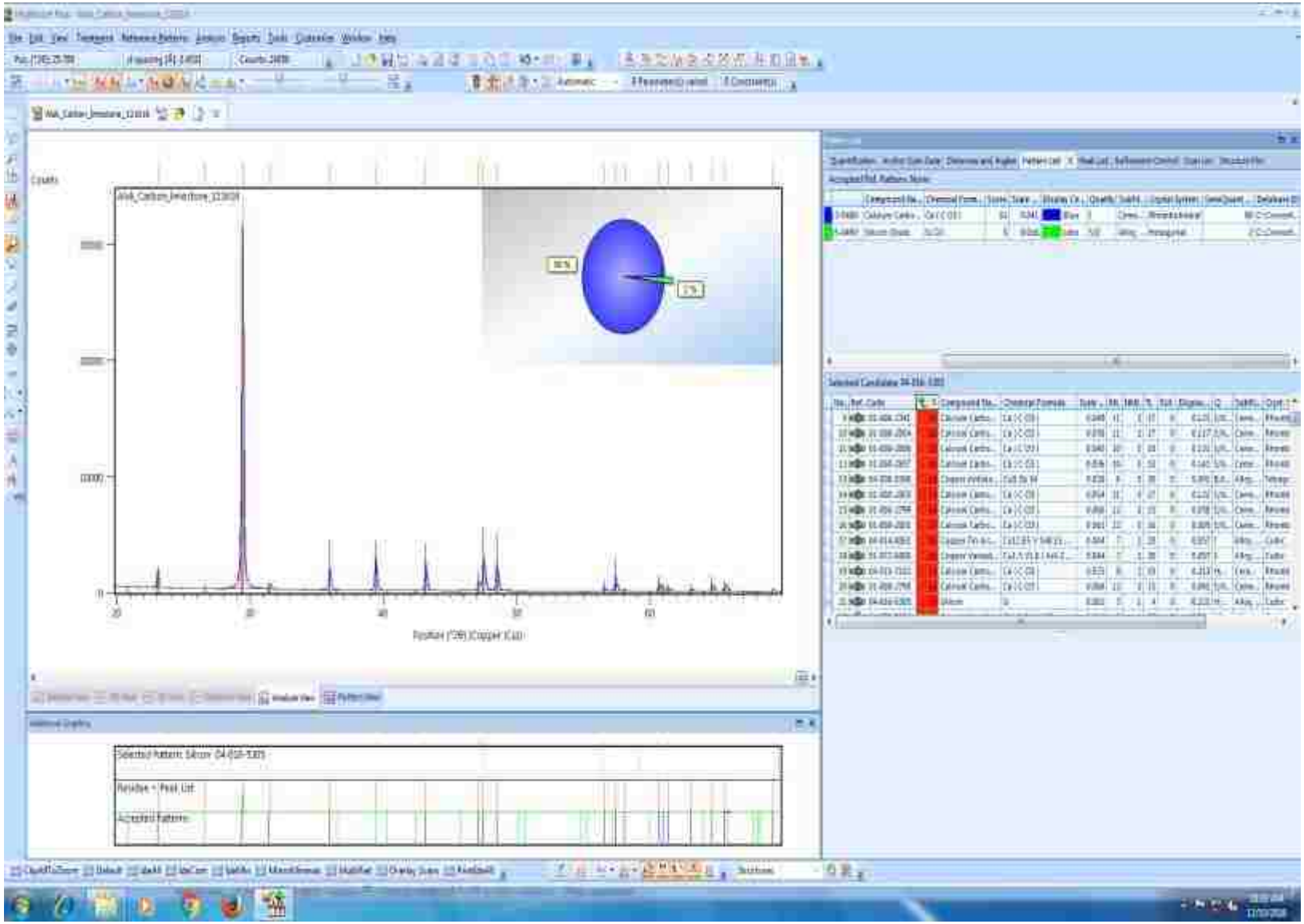

APPENDIX C: TECHNICAL DATA SHEET FOR THE EPOXY USED

The following set of images are screenshots of the technical data sheet from the manufacturer of the Epoxy used to seal the model

HEXION
Technical Data Sheet

Re-issued September 2005

EPON™ Resin 828

Product Description

EPON™ Resin 828 is an undiluted clear difunctional bisphenol A/epichlorohydrin derived liquid epoxy resin. When cross-linked or hardened with appropriate curing agents, very good mechanical, adhesive, dielectric and chemical resistance properties are obtained. Because of this versatility, EPON Resin 828 has become a standard epoxy resin used in formulation, fabrication and fusion technology.

Benefits

- Fiber reinforced pipes, tanks and composites
- Tooling, casting and molding compounds
- Construction, electrical and aerospace adhesives
- High solids/low VOC maintenance and marine coatings
- Electrical encapsulations and laminates
- Chemical resistant tank linings, flooring and grouts
- Base resin for epoxy fusion technology

Sales Specification

Property	Units	Value	Test Method/Standard
Weight per Epoxide	g/eq	185 – 192	ASTM D1652
Viscosity at 25°C	P	110 – 150	ASTM D445
Color	Gardner	1 max.	ASTM D1544

Typical Properties

Property	Units	Value	Test Method/Standard
Density at 25°C	lb/gal	9.7	ASTM D1475
Density at 25°C	g/ml	1.16	
Vapor pressure @ 25°C (77°F)	mm Hg	0.03	
Refractive index @ 25°C (77°F)		1.573	
Specific heat	BTU/lb/°F	0.5	

Processing/How to use

General Information

EPON Resin 828

The low viscosity and cure properties of EPON Resin 828 allow its use under various application and fabrication techniques including:

• Spraying and brushing	• Pultrusion
• Filament winding	• Casting
• Pressure laminating	• Molding
• Vacuum bag laminating	• Toweling

Curing Agents

EPON Resin 828 can be cured or cross-linked with a variety of curing agents depending on properties desired in the finished product and the processing conditions employed. Some commonly used curing agents, recommended concentrations, typical cure schedules employed in major end-use applications, plus sources for these curing agents are displayed in Table 1.

Performance Properties

Performance Characteristics of Cured EPON Resin 828

Mechanical Properties

High performance, high strength materials are obtained when this resin is cured with a variety of curing agents. Unfilled systems in common use have tensile values greater than 10,000 psi (69 MPa) with modulus values greater than 400,000 psi (2750 MPa). Such systems are normally very rigid. If greater flexibility is needed systems can be formulated to provide up to 300% elongation.

Adhesive Properties

One of the most widely recognized properties of cured EPON Resin 828 is strong adhesion to a broad range of substrates. Such systems exhibit shear strength of up to 6,000 psi (41 Mpa). One factor which contributes to this property is the low shrinkage shown by these systems during cure. Compared to other polymers, epoxy resins have low internal stresses resulting in strong and durable finished products.

Electrical Properties

EPON Resin 828 cured systems have very good electrical insulating characteristics and dielectric properties. For example, systems can be obtained with anhydride and amine curing agents having volume resistivities up to 1 x 10E16 ohm-cm, dielectric constants of 3-5 and dissipation factors of 0.002 to 0.020 at ambient conditions. Electrical encapsulations, laminates and molding compounds are frequently based on EPON Resin 828.

Chemical Resistance

Cured EPON Resin 828 is highly resistant to a broad range of chemicals, including caustic, acids, fuels and solvents. Chemically resistant reinforced structures and linings or coatings over metal can be formulated with EPON Resin 828.

Formulating Techniques

The primary components of a thermosetting resin formula are the epoxy resin and the hardener or curing agent. However, in practice other materials are normally incorporated to achieve special properties. For example, inert fillers such as silicas, talcs, calcium silicates, micas, clays and calcium carbonate can be added to further reduce shrinkage and improve dimensional stability. Also, reactive diluents can be added to EPON Resin 828 to reduce viscosity. The effect on viscosity by adding such

materials is shown in Figure 1.

Table 1 / **Curing Agents for EPON™ 828**

Curing Agent[1]	Physical State	Recommended Concentration Range, phr[2]	Typical Cure Schedule Time °C (°F)	Deflection Temperature °C (°F)	Applications[3]	Supplier[4]
Aliphatic Amines						
EPIKURE™ 3223 (DETA)	Liquid	12	7d, 25(77)	120(250)	ABCDEFHI	5
EPIKURE 3234 (TETA)	Liquid	13	7d, 25(77)	120(250)	ABCDEFHI	5
EPIKURE 3200 (AEP)	Liquid	22	24h, 25(77) & 1h, 150(300)	120(250)	BCEFGH	5
EPIKURE 3270	Liquid	75	14d, 25(77)	56(133)	ABCDEFHI	5
EPIKURE 3271	Liquid	18	14d, 25(77)	66(151)	ABCDEFHI	5
EPIKURE 3274	Liquid	40	14d, 25(77)	—	ABCDEFHI	5
EPIKURE 3230	Liquid	35	7d, 25(77)	68(155)	ABCDEFHI	1
D-400 Type PEA	Liquid	55	30 min, 115 (240)	31(88)	ABCEFH	1
Cycloaliphatic Amines						
EPIKURE 3370	Liquid	38	7d, 25(77)	56(133)	ABCDEFHI	5
EPIKURE 3382	Liquid	63	7d, 25(77)	63(145)	ABCDEFHI	5
EPIKURE 3383	Liquid	60	24h, 25(77) & 2h, 100(212)	54(129)	ABCDEFHI	5
Polyamides						
EPIKURE 3115	Liquid	120	1h, 100(212)	85(185)	AB	5
EPIKURE 3125	Liquid	90	7d, 25(77)	90(195)	ABCEFH	5
EPIKURE 3140	Liquid	75	7d, 25(77)	115(240)	ABCEFH	5
Amidoamines						
EPIKURE 3015	Liquid	50	16h, 25(77) & 2h, 93(200)	—	ABCDEFHI	5
EPIKURE 3055	Liquid	50	16h, 25(77) & 2h, 93(200)	67(153)	ABCDEFHI	5
EPIKURE 3072	Liquid	35	14d, 25(77)	59(138)	ABCDEFHI	5

APPENDIX D: RAW DATA FROM THE GAGD EXPERIMENTAL RUNS FOR NITROGEN INJECTION AT 5 CC/MIN FOR MODEL # 1

Time (min)	Gas Injected (cc)	Vol water	Run N_5_1 Vol oil	Cum vol	Run N_5_1 % Recovery
0	0	50	0	50	0.00%
0.5	2.5	50	25	75	2.44%
1	5	52	38	90	3.71%
1.5	7.5	53	49	102	4.78%
2	10	53	62	115	6.05%
2.5	12.5	55	65	120	6.34%
3	15	55	70	125	6.83%
3.5	17.5	55	80	135	7.80%
4	20	55	90	145	8.78%
4.5	22.5	55	93	148	9.07%
5	25	55	97	152	9.46%
5.5	27.5	55	102	157	9.95%
6	30	55	108	163	10.54%
6.5	32.5	55	115	170	11.22%
7	35	55	120	175	11.71%
7.5	37.5	55	125	180	12.20%
8	40	55	130	185	12.68%
8.5	42.5	55	133	188	12.98%
9	45	55	138	193	13.46%
9.5	47.5	55	142	197	13.85%
10	50	55	145	200	14.15%
10.5	52.5	55	149	204	14.54%
11	55	55	153	208	14.93%
11.5	57.5	55	157	212	15.32%
12	60	55	160	215	15.61%
12.5	62.5	55	164	219	16.00%
13	65	55	167	222	16.29%
13.5	67.5	55	170	225	16.59%
14	70	55	173	228	16.88%
14.5	72.5	55	176	231	17.17%
15	75	55	179	234	17.46%
15.5	77.5	55	182	237	17.76%
16	80	55	185	240	18.05%
16.5	82.5	55	189	244	18.44%
17	85	55	193	248	18.83%
17.5	87.5	55	195	250	19.02%
18	90	55	198	253	19.22%
18.5	92.5	55	202	257	19.71%
19	95	55	206	261	20.10%
19.5	97.5	55	209	264	20.39%
20	100	55	213	268	20.78%
20.5	102.5	55	215	270	20.98%
21	105	55	219	274	21.37%
21.5	107.5	55	222	277	21.66%
22	110	55	225	280	21.95%
22.5	112.5	55	228	283	22.24%
23	115	55	231	286	22.54%

Time (min)	Gas Injected (cc)	Vol water	Run N_5_1 Vol oil	Cum vol	Run N_5_1 % Recovery
45.5	227.5	55	376	431	36.68%
46	230	55	380	435	37.07%
46.5	232.5	55	383	438	37.37%
47	235	55	387	442	37.76%
47.5	237.5	55	389	444	37.95%
48	240	55	391	446	38.15%
48.5	242.5	55	395	450	38.54%
49	245	55	398	453	38.83%
49.5	247.5	55	403	457	39.22%
50	250	55	405	460	39.51%
50.5	252.5	55	408	463	39.80%
51	255	55	411	466	40.10%
51.5	257.5	55	415	470	40.49%
52	260	55	419	474	40.88%
52.5	262.5	55	421	476	41.07%
53	265	55	425	480	41.46%
53.5	267.5	55	429	484	41.85%
54	270	55	433	487	42.15%
54.5	272.5	55	436	491	42.54%
55	275	55	440	495	42.93%
55.5	277.5	55	443	498	43.22%
56	280	50	445	52	43.41%
56.5	282.5	50	448	55	43.71%
57	285	50	451	58	44.00%
57.5	287.5	50	455	62	44.39%
58	290	50	457	64	44.59%
58.5	292.5	50	460	67	44.88%
59	295	50	463	70	45.17%
59.5	297.5	50	466	73	45.46%
60	300	50	469	76	45.76%
60.5	302.5	50	472	79	46.05%
61	305	50	475	82	46.34%
61.5	307.5	50	476	83	46.44%
62	310	50	478	85	46.63%
62.5	312.5	50	481	88	46.93%
63	315	50	485	92	47.32%
63.5	317.5	50	491	98	47.90%
64	320	50	495	102	48.29%
64.5	322.5	50	499	106	48.68%
65	325	50	503	110	49.07%
65.5	327.5	50	507	114	49.46%
66	330	50	511	118	49.85%
66.5	332.5	50	515	122	50.24%
67	335	50	518	125	50.54%
67.5	337.5	50	521	128	50.83%
68	340	50	524	131	51.12%
68.5	342.5	50	527	134	51.41%

Time (min)	Gas Injected (cc)	Vol water	Run N_5_1 Vol oil	Cum vol	Run N_5_1 % Recovery
90.5	452.5	50	661	268	54.49%
91	455	50	664	271	64.78%
91.5	457.5	50	668	275	65.17%
92	460	50	670	277	65.37%
92.5	462.5	50	673	280	65.66%
93	465	50	675.5	282.5	65.90%
93.5	467.5	50	678	285	66.15%
94	470	50	681	288	66.44%
94.5	472.5	50	683	290	66.63%
95	475	50	685.5	292.5	66.88%
95.5	477.5	50	688	295	67.12%
96	480	50	690.5	297.5	67.37%
96.5	482.5	50	693	300	67.61%
97	485	50	695	302	67.80%
97.5	487.5	50	696	303	67.90%
98	490	52	696	305	67.90%
98.5	492.5	52	697.5	306.5	68.05%
99	495	52	699	308	68.20%
99.5	497.5	52	699.5	308.5	68.24%
100	500	52	701	310	68.39%
100.5	502.5	52	701	310	68.39%
101	505	52	701	310	68.39%
101.5	507.5	52	701	310	68.39%
102	510	52	703	312	68.59%
102.5	512.5	54	704	315	68.68%
103	515	55	704	316	68.68%
103.5	517.5	55	704	316	68.68%
104	520	56.5	704	317.5	68.68%
104.5	522.5	56.5	705.5	319	68.83%
105	525	57.5	705.5	320	68.83%
105.5	527.5	57.5	705.5	320	68.83%
106	530	57.5	705.5	320	68.83%
106.5	532.5	57.5	705.5	320	68.83%
107	535	57.5	705.5	320	68.83%
107.5	537.5	57.5	705.5	320	68.83%
108	540	57.5	705.5	320	68.83%
108.5	542.5	57.5	705.5	320	68.83%
109	545	57.5	705.5	320	68.83%
109.5	547.5	58.5	705.5	321	68.83%
110	550	59.5	705.5	322	68.81%
110.5	552.5	60	706.5	323.5	68.93%
111	555	60.5	707.5	325	69.02%
111.5	557.5	60.5	709	326.5	69.17%
112	560	60.5	710.5	328	69.32%
112.5	562.5	60.5	714.5	329	69.41%
113	565	60.5	712.5	330	69.51%
113.5	567.5	60.5	713	330.5	69.56%

23.5	117.5	55	235	290	22.93%
24	120	55	238	293	23.22%
24.5	122.5	55	241	296	23.51%
25	125	55	243	298	23.71%
25.5	127.5	55	246	301	24.00%
26	130	55	249	304	24.29%
26.5	132.5	55	253	308	24.68%
27	135	55	256	311	24.98%
27.5	137.5	55	260	315	25.37%
28	140	55	264	319	25.76%
28.5	142.5	55	267	322	26.05%
29	145	55	271	326	26.44%
29.5	147.5	55	274	329	26.73%
30	150	55	278	333	27.12%
30.5	152.5	55	281	336	27.41%
31	155	55	283	338	27.61%
31.5	157.5	55	286	341	27.90%
32	160	55	289	344	28.20%
32.5	162.5	55	293	348	28.59%
33	165	55	296	351	28.88%
33.5	167.5	55	300	355	29.27%
34	170	55	303	358	29.56%
34.5	172.5	55	307	362	29.95%
35	175	55	310	365	30.24%
35.5	177.5	55	313	368	30.54%
36	180	55	316	371	30.83%
36.5	182.5	55	320	375	31.22%
37	185	55	323	378	31.51%
37.5	187.5	55	326	381	31.80%
38	190	55	330	385	32.20%
38.5	192.5	55	333	388	32.49%
39	195	55	336	391	32.78%
39.5	197.5	55	339	394	33.07%
40	200	55	343	398	33.46%
40.5	202.5	55	346	401	33.76%
41	205	55	348	403	33.95%
41.5	207.5	55	351	406	34.24%
42	210	55	354	409	34.54%
42.5	212.5	55	357	412	34.83%
43	215	55	360	415	35.12%
43.5	217.5	55	364	419	35.51%
44	220	55	368	423	35.90%
44.5	222.5	55	370	425	36.10%
45	225	55	373	428	36.39%

69	345	50	529	136	51.61%
69.5	347.5	50	533	140	52.00%
70	350	50	536	143	52.29%
70.5	352.5	50	538	145	52.49%
71	355	50	541	148	52.78%
71.5	357.5	50	544	151	53.07%
72	360	50	548	155	53.46%
72.5	362.5	50	551	158	53.76%
73	365	50	553	160	53.95%
73.5	367.5	50	556	163	54.24%
74	370	50	559	166	54.54%
74.5	372.5	50	563	170	54.93%
75	375	50	565	172	55.12%
75.5	377.5	50	570	177	55.61%
76	380	50	573	180	55.90%
76.5	382.5	50	578	185	56.39%
77	385	50	581	188	56.68%
77.5	387.5	50	584	191	56.98%
78	390	50	588	195	57.37%
78.5	392.5	50	591.5	198.5	57.71%
79	395	50	594	201	57.95%
79.5	397.5	50	597	204	58.24%
80	400	50	600.5	207.5	58.59%
80.5	402.5	50	603	210	58.83%
81	405	50	605.5	212.5	59.07%
81.5	407.5	50	608	215	59.32%
82	410	50	612	219	59.71%
82.5	412.5	50	615	222	60.00%
83	415	50	618	225	60.29%
83.5	417.5	50	620.5	227.5	60.54%
84	420	50	623.5	230.5	60.83%
84.5	422.5	50	626	233	61.07%
85	425	50	629	236	61.37%
85.5	427.5	50	631.5	238.5	61.61%
86	430	50	634.5	241.5	61.90%
86.5	432.5	50	638	245	62.24%
87	435	50	641.5	248.5	62.59%
87.5	437.5	50	644	251	62.83%
88	440	50	648	255	63.22%
88.5	442.5	50	650.5	257.5	63.46%
89	445	50	653	260	63.71%
89.5	447.5	50	655.5	262.5	63.95%
90	450	50	658	265	64.20%

114	570	60.5	713.5	331	69.61%
114.5	572.5	60.5	714	331.5	69.66%
115	575	60.5	714.5	332	69.71%
115.5	577.5	60.5	714.5	332	69.71%
116	580	60.5	714.5	332	69.71%
116.5	582.5	60.5	714.5	332	69.71%
117	585	60.5	714.5	332	69.71%
117.5	587.5	60.5	715	332.5	69.76%
118	590	60.5	715.5	333	69.80%
118.5	592.5	60.5	716	333.5	69.85%
119	595	60.5	716.5	334	69.90%
119.5	597.5	60.5	717	334.5	69.95%
120	600	60.5	717.5	335	70.00%
125	625	60.5	720.5	338	70.29%
130	650	60.5	722.5	340	70.49%
135	675	60.5	724	341.5	70.63%
140	700	60.5	726.5	344	70.88%
145	725	60.5	728.5	346	71.07%
150	750	60.5	732.5	350	71.46%
155	775	60.5	733	350.5	71.51%
160	800	60.5	734	351.5	71.61%
165	825	60.5	736.5	354	71.85%
170	850	60.5	737.5	355	71.95%
175	875	60.5	738.5	356	72.05%
180	900	60.5	740.5	358	72.24%
195	975	50	748.5	58	73.02%
210	1050	50	752.5	62	73.41%
225	1125	50	755.5	65	73.71%
240	1200	50	758.5	68	74.00%
255	1275	50	761.5	71	74.29%
270	1350	50	765.5	75	74.68%
285	1425	50	766.5	76	74.78%
300	1500	50	770.5	80	75.17%
330	1650	50	785.5	95	76.63%
360	1800	50	805.5	115	78.59%
390	1950	50	809.5	119	78.98%
420	2100	50	812.5	122	79.27%
450	2250	50	816.5	126	79.66%
480	2400	50	818.5	128	79.85%
510	2550	50	819.5	129	79.95%
540	2700	50	820.5	130	80.05%

APPENDIX E: RAW DATA FROM THE GAGD EXPERIMENTAL RUNS FOR NITROGEN INJECTION AT 5 CC/MIN FOR MODEL # 2

Time (min)	Gas Injected (cc)	Vol water	Run 2N_5_1 Vol oil	Cum vol	Run 2N_5_1 % Recovery
0	0	50	0	50	0.00%
0.5	2.5	51	14	65	1.47%
1	5	52	22	74	2.32%
1.5	7.5	54	28	82	2.95%
2	10	55	38	93	4.00%
2.5	12.5	56	45	101	4.74%
3	15	57	52	109	5.47%
3.5	17.5	58	60	118	6.32%
4	20	60	67	127	7.05%
4.5	22.5	60	77	137	8.11%
5	25	60	86	146	9.05%
5.5	27.5	60	95	155	10.00%
6	30	60	104	164	10.95%
6.5	32.5	60	112	172	11.79%
7	35	60	121	181	12.74%
7.5	37.5	60	130	190	13.68%
8	40	60	139	199	14.63%
8.5	42.5	61	146	207	15.37%
9	45	61	154	215	16.21%
9.5	47.5	61	163	224	17.16%
10	50	61	172	233	18.11%
10.5	52.5	61	181	242	19.05%
11	55	61	190	251	20.00%
11.5	57.5	61	198	259	20.84%
12	60	61	206	267	21.68%
12.5	62.5	61	214	275	22.53%
13	65	61	222	283	23.37%
13.5	67.5	61	230	291	24.21%
14	70	61	236	297	24.84%
14.5	72.5	61	242	303	25.47%
15	75	61	248	309	26.11%
15.5	77.5	62	254	316	26.74%
16	80	63	260	323	27.37%
16.5	82.5	63	267	330	28.11%
17	85	64	274	338	28.84%
17.5	87.5	64	281	345	29.58%
18	90	64	288	352	30.32%
18.5	92.5	64	295	359	31.05%
19	95	64	302	366	31.79%
19.5	97.5	65	309	374	32.53%
20	100	65	316	381	33.26%
20.5	102.5	65	323	388	34.00%
21	105	65	331	396	34.84%
21.5	107.5	65	338	403	35.58%
22	110	65	345	410	36.32%
22.5	112.5	65	351	416	36.95%
23	115	65	357	422	37.58%

Time (min)	Gas Injected (cc)	Vol water	Run 2N_5_1 Vol oil	Cum vol	Run 2N_5_1 % Recovery
45.5	227.5	54	661	777	69.58%
46	230	54	666	782	70.11%
46.5	232.5	54	671	787	70.63%
47	235	54	676	792	71.16%
47.5	237.5	54	681	797	71.68%
48	240	55	686	803	72.21%
48.5	242.5	55	691	808	72.74%
49	245	55	696	813	73.26%
49.5	247.5	55	701	818	73.79%
50	250	55	705	822	74.21%
50.5	252.5	55	709	826	74.63%
51	255	55	712	829	74.95%
51.5	257.5	55	715	832	75.26%
52	260	55	718	835	75.58%
52.5	262.5	55	721	838	75.89%
53	265	55	724	841	76.21%
53.5	267.5	55	727	844	76.53%
54	270	55	730	847	76.84%
54.5	272.5	55	733	850	77.16%
55	275	56	734	852	77.26%
55.5	277.5	56	736	854	77.47%
56	280	56	737	855	77.58%
56.5	282.5	57	737	856	77.58%
57	285	57	737	856	77.58%
57.5	287.5	57.5	737	856.5	77.58%
58	290	57.5	737	856.5	77.58%
58.5	292.5	58	737	857	77.58%
59	295	58	737	857	77.58%
59.5	297.5	58	737	857	77.58%
60	300	59	737	858	77.68%
60.5	302.5	60	738	860	77.68%
61	305	60	738	860	77.68%
61.5	307.5	60	738	860	77.68%
62	310	60	738.5	860.5	77.74%
62.5	312.5	60	738.5	860.5	77.74%
63	315	60	739	861	77.79%
63.5	317.5	60	739	861	77.79%
64	320	64	739	865	77.79%
64.5	322.5	65	739	866	77.79%
65	325	65	740	867	77.89%
65.5	327.5	65	740	867	77.89%
66	330	65	740.5	867.5	77.95%
66.5	332.5	65	741	868	78.00%
67	335	65	741	868	78.00%
67.5	337.5	65	741	868	78.00%
68	340	65	741	868	78.00%
68.5	342.5	65	741.5	868.5	78.05%

Time (min)	Gas Injected (cc)	Vol water	Run 2N_5_1 Vol oil	Cum vol	Run 2N_5_1 % Recovery
90.5	452.5	75	742	879	78.11%
91	455	75	742	879	78.11%
91.5	457.5	75	742	879	78.11%
92	460	75	743	880	78.21%
92.5	462.5	75	745	882	78.42%
93	465	75	745	882	78.42%
93.5	467.5	75	745.5	882.5	78.47%
94	470	75	746	883	78.53%
94.5	472.5	75	746	883	78.53%
95	475	75	746	883	78.53%
95.5	477.5	75	746.5	883.5	78.58%
96	480	75	746.5	883.5	78.58%
96.5	482.5	75	746.5	883.5	78.58%
97	485	75	747	884	78.63%
97.5	487.5	75	747	884	78.63%
98	490	75	747	884	78.63%
98.5	492.5	75	747	884	78.63%
99	495	75	748	885	78.74%
99.5	497.5	75	748.5	885.5	78.79%
100	500	75	749	886	78.84%
100.5	502.5	75	749.5	886.5	78.89%
101	505	75	750	887	78.95%
101.5	507.5	75	751	888	79.05%
102	510	75	751.5	888.5	79.11%
102.5	512.5	75	752	889	79.16%
103	515	75	752.5	889.5	79.21%
103.5	517.5	75	752.5	889.5	79.21%
104	520	75	753	890	79.26%
104.5	522.5	75	753	890	79.26%
105	525	75	754	891	79.37%
105.5	527.5	75	754	891	79.37%
106	530	75	754.5	891.5	79.42%
106.5	532.5	75	754.5	891.5	79.42%
107	535	75	755	892	79.47%
107.5	537.5	75	755.5	892.5	79.53%
108	540	75	756	893	79.58%
108.5	542.5	75	756.5	893.5	79.63%
109	545	75	757	894	79.68%
109.5	547.5	75	757.5	894.5	79.74%
110	550	75	758	895	79.79%
110.5	552.5	75	759	896	79.89%
111	555	75	759.5	896.5	79.95%
111.5	557.5	75	759.5	896.5	79.95%
112	560	75	760	897	80.00%
112.5	562.5	75	760.5	897.5	80.05%
113	565	75	761	898	80.11%
113.5	567.5	75	761.5	898.5	80.16%

23.5	117.5	65	364	429	38.32%
24	120	65	372	437	39.16%
24.5	122.5	65	379	444	39.89%
25	125	65	386	451	40.63%
25.5	127.5	65	393	458	41.37%
26	130	65	401	466	42.21%
26.5	132.5	65	408	473	42.95%
27	135	65	415	480	43.68%
27.5	137.5	65	423	488	44.53%
28	140	65	431	496	45.37%
28.5	142.5	65	438	503	46.11%
29	145	50	445	57	46.84%
29.5	147.5	50	453	65	47.68%
30	150	50	460	72	48.42%
30.5	152.5	50	468	80	49.26%
31	155	50	475	87	50.00%
31.5	157.5	50	483	95	50.84%
32	160	50	491	103	51.68%
32.5	162.5	50	498	110	52.42%
33	165	50	506	118	53.26%
33.5	167.5	50	514	126	54.11%
34	170	50	521	133	54.84%
34.5	172.5	50	528	140	55.58%
35	175	50	534	146	56.21%
35.5	177.5	50	540	152	56.84%
36	180	50	548	160	57.68%
36.5	182.5	50	555	167	58.42%
37	185	50	561	173	59.05%
37.5	187.5	50	569	181	59.89%
38	190	50	576	188	60.63%
38.5	192.5	50	583	195	61.37%
39	195	50	590	202	62.11%
39.5	197.5	51	596	209	62.74%
40	200	50	604	216	63.58%
40.5	202.5	52	608	222	64.00%
41	205	53	614	229	64.63%
41.5	207.5	53	621	236	65.37%
42	210	53	628	243	66.11%
42.5	212.5	53	634	249	66.74%
43	215	54	638	254	67.16%
43.5	217.5	54	643	259	67.68%
44	220	54	648	264	68.21%
44.5	222.5	54	653	269	68.74%
45	225	54	657	273	69.16%

69	345	65	741.5	368.5	78.05%
69.5	347.5	65	742	369	78.11%
70	350	65	742	369	78.11%
70.5	352.5	65	742	369	78.11%
71	355	65	742.5	369.5	78.16%
71.5	357.5	65	743	370	78.21%
72	360	65	743	370	78.21%
72.5	362.5	65	743	370	78.21%
73	365	65	743	370	78.21%
73.5	367.5	65	743	370	78.21%
74	370	65	743	370	78.21%
74.5	372.5	65	744	371	78.32%
75	375	65	744	371	78.32%
75.5	377.5	66	744	372	78.32%
76	380	69	745	376	78.42%
76.5	382.5	72	746	380	78.53%
77	385	73	746	381	78.53%
77.5	387.5	75	747	384	78.63%
78	390	75	747	384	78.63%
78.5	392.5	75	735.5	372.5	77.42%
79	395	75	736	373	77.47%
79.5	397.5	75	736	373	77.47%
80	400	75	736.5	373.5	77.53%
80.5	402.5	75	737	374	77.58%
81	405	75	737	374	77.58%
81.5	407.5	75	737.5	374.5	77.63%
82	410	75	737.5	374.5	77.63%
82.5	412.5	75	737.5	374.5	77.63%
83	415	75	737.5	374.5	77.63%
83.5	417.5	75	737.5	374.5	77.63%
84	420	75	738	375	77.68%
84.5	422.5	75	738	375	77.68%
85	425	75	738	375	77.68%
85.5	427.5	75	738	375	77.68%
86	430	75	738	375	77.68%
86.5	432.5	75	739	376	77.79%
87	435	75	739	376	77.79%
87.5	437.5	75	739.5	376.5	77.84%
88	440	75	739.5	376.5	77.84%
88.5	442.5	75	740	377	77.89%
89	445	75	740	377	77.89%
89.5	447.5	75	741	378	78.00%
90	450	75	741.5	378.5	78.05%

114	570	75	761.5	398.5	80.16%
114.5	572.5	75	762	399	80.21%
115	575	75	762	399	80.21%
115.5	577.5	75	762.5	399.5	80.26%
116	580	75	762.5	399.5	80.26%
116.5	582.5	75	763	400	80.32%
117	585	75	763.5	400.5	80.37%
117.5	587.5	75	763.5	400.5	80.37%
118	590	75	764	401	80.42%
118.5	592.5	75	765	402	80.53%
119	595	75	766	403	80.63%
119.5	597.5	75	766.5	403.5	80.68%
120	600	75	766.5	403.5	80.68%
125	625	75	768	405	80.84%
130	650	75	771	408	81.16%
135	675	75	773.5	410.5	81.42%
140	700	75	775.5	412.5	81.63%
145	725	75	778	415	81.89%
150	750	75	780.5	417.5	82.16%
155	775	75	782	419	82.32%
160	800	75	784	421	82.53%
165	825	75	785.5	422.5	82.68%
170	850	75	787	424	82.84%
175	875	75	788	425	82.95%
180	900	75	789.5	426.5	83.11%
195	975	75	793	430	83.47%
210	1050	75	796	433	83.79%
225	1125	75	799	436	84.11%
240	1200	75	801.5	438.5	84.37%
255	1275	75	804	441	84.63%
270	1350	75	807	444	84.95%
285	1425	75	809.5	446.5	85.21%
300	1500	75	812	449	85.47%
330	1650	75	815	452	85.79%
360	1800	75	821	458	86.42%
390	1950	75	825	462	86.84%
420	2100	75	828	465	87.16%
450	2250	75	831	468	87.47%
480	2400	75	832	469	87.58%
510	2550	75	833	470	87.68%
540	2700	75	833	470	87.68%

VITA

Alok Shah is the son of Jitesh and Kumud Shah. He was born in Gujarat, India. He attended schools in India up to high school. He began his high school in the USA in Georgia and went on to earn a Bachelors of Science (BS) in Environmental Engineering from the University of Georgia (Athens, GA) in 2013. After working for a year at a research facility for the Environmental Protection Agency (EPA), he enrolled in the Master of Science program in petroleum engineering at the Louisiana State University and A&M College in fall 2014. Alok has also been working as a project engineer with CH2M since May 2016 while working on his masters.